NRC·CNRC Aerospace

Review of Aeronautical Fatigue and Structural Integrity Work in Canada (2021 – 2023)

Editor: Min Liao

Report No.: LTR-SMM-2023-0112
RDIMS No.: N/A
Date: June 2023

National Research Council Canada | Conseil national de recherches Canada

Canada

NATIONAL RESEARCH COUNCIL CANADA (NRC)

AEROSPACE

Review of Aeronautical Fatigue and Structural Integrity Work in Canada (2021 – 2023)

Volume 1 of 1

Report No.: LTR-SMM-2023-0112

RDIMS No.: N/A

Date: June 2023

Editor: Min Liao

Classification:	Unclassified	Distribution:	Unlimited
For:	International Committee on Aeronautical Fatigue and Structural Integrity (ICAF)		
Reference:	-		
Submitted by:	Dr. Rick Kearsey, Director/A, Structures and Materials Performance Laboratory		
Approved by:	Dr. Mouhab Meshreki, Director in General, Aerospace Research Center		

Pages:	80	Copy No.:	N/A
Figures:	68	Tables:	2

EXECUTIVE SUMMARY

This report provides a review of aeronautical fatigue and structural integrity work carried out in Canada during the period from April 2021 to April 2023. The review is a collection of multiple work summaries that were provided by Canadian industrial partners, universities, and government organizations. All aspects of structural integrity, especially fatigue related work, including: full-scale testing with environmental effects, aircraft structural integrity program and fleet management, life assessment and enhancement, load and usage monitoring, structural health monitoring, non-destructive inspection, and new material and manufacturing, are covered in this report.

This national review will be presented at the 38th Conference and 31st Symposium of the International Committee on Aeronautical Fatigue and Structural Integrity (https://www.icaf2023.nl/) on 26 – 29 June 2023, Delft, The Netherlands. The whole report will be archived on the ICAF permanent website (https://www.icaf.aero/index.php).

The page is left blank intentionally

TABLE OF CONTENTS

LIST OF FIGURES

LIST OF TABLES

1.0 INTRODUCTION

As a part of the National Review for the International Committee on Aeronautical Fatigue and Structural Integrity (ICAF), Canadian industrial partners, universities and government agencies were solicited for information describing their fatigue technology and structural integrity related activities over the period from April 2021 to April 2023. This review covers work performed or being performed by the following organizations (including some non-Canadian collaborative organizations):

- L3Harris - Military Aircraft Services (MAS)
- Cranfield University, UK
    - School of Aerospace, Transport and Manufacturing
- Carleton University
    - Department of Mechanical and Aerospace Engineering
- Laval University
    - Department of Electrical and Computer Engineering
- Queen's University
- Royal Military College of Canada (RMC)
- Toronto Metropolitan University
    - Department of Mechanical and Industrial Engineering
- University of British Columbia (UBC)
    - Intelligent Sensing, Diagnostics, and Prognostics Research Lab
- York University
    - Department of Mechanical Engineering, Lassonde School of Engineering
- Department of National Defence (DND)
    - Defence Research and Development Canada (DRDC)
    - Directorate of Technical Airworthiness and Engineering Support (DTAES)
    - Quality Engineering Test Establishment (QETE)
    - Royal Canadian Air Force (RCAF)
- National Research Council of Canada (NRC)
    - Aerospace Research Centre (NRC Aerospace)
    - Digital Technology Research Center (DTRC)

Names of contributors (where available) and their organizations are included in the text of this review. The full addresses of the contributors are available through the ICAF Canadian National Delegate whose contact is at the end of this section.

For ease of reading, this review report is organised based on the following main topics:

- Full-Scale Structural and Component Testing;
- Aircraft Structural Integrity Program and Fleet Management;
- Fatigue Life Assessment and Enhancement Technologies;
- Load, Usage, and Structural Health Monitoring;
- Non-Destructive Evaluation;
- Fatigue and Structural Integrity of Composite; and
- Fatigue and Structure Integrity of New Materials.

References are provided after each individual work summary, which includes more details of the reported work. For questions on this report, you may contact the individual contributor and/or the Canadian National Delegate at:

Dr. Min Liao, Principal Research Officer
Group Leader - Structural Integrity
Aerospace, National Research Council Canada
1200 Montreal Road, Building M14
Ottawa, ON, K1A 0R6, Canada
Email: Min.Liao@nrc-cnrc.gc.ca

2.0 FULL-SCALE STRUCTURAL AND COMPONENT TESTING

2.1 Experimental Strength and Fatigue Assessment of a Disbonded F/A-18A/B/C/D Inner Wing Step Lap Joint*

Eric Dionne, NRC Aerospace
* Full paper being presented at ICAF2023

The National Research Council of Canada (NRC) is carrying out a test campaign on a disbonded F/A-18A/B/C/D Inner Wing Step Lap Joint (IWSLJ) in collaboration with the Royal Canadian Air Force, armasuisse, the United States Navy, RUAG, and L3 Harris.

Many disbonds have been reported by the F/A-18A/B/C/D fleet operators. The majority of the disbonds found are small relative to the size of the IWSLJ. The immediate effects of those disbonds and their changes in a long term are not well understood. The NRC is conducting a full-scale test (see Figure 1) aimed at better understanding the effects of a partially disbonded IWSLJ on the F/A-18 wing structural integrity.

2.1.1 RESIDUAL STRENGTH

One of the primary purposes of this test is to evaluate the residual strength of a partially disbonded Stepped Lap Joint (SLJ) of the lower wing skin. For this purpose, the United States Navy donated a retired wing with a pre-existing disbond similar to those found in the F/A-18A/B/C/D fleet (see Figure 2). Static loads will be applied to the test article to demonstrate sufficient residual strength in presence of the small disbond. The test is performed at Room Temperature (RT) and loads are scaled up for temperature effects; this allows for a simpler test setup.

2.1.2 EFFECT OF CONSTANT AMPLITUDE LOADING

The second aim is to try to generate damage growth data for a common size of disbond in the SLJ. Repeated constant amplitude loads will be applied in an attempt to grow the disbond. The loads will be progressively increased and the disbond will be frequently inspected using customized non-destructive inspection techniques able to detect and measure disbond size and quantify the resulting growth. The data from the numerous sensors will also be monitored to detect if the disbond growth can be measured in a test environment.

2.1.3 LOAD REDISTRIBUTION

The third aim is to evaluate the internal load distribution as a result of the disbond growth. The test article is equipped with over 250 strain gauges on the SLJ, as well as, on the surrounding structure as it is believed that new load paths will be created as the disbond grows. Digital Image Correlation (DIC) is also used on both the upper and lower SLJ with the anticipation it would detect a perturbation of the strain field at the tip of the disbond. Fiber optic sensors were also

installed along the spars to detect load bypassing from the skin to spar caps. The sensor measurements will also be correlated to a Finite Element (FE) model of the wing in an effort to enable the development of FE models to replicate and predict more complex disbond scenarios.

All testing is carried out at the Structural Integrity Laboratory, Building M-14, NRC Aerospace Research Centre, Montreal Road Campus in Ottawa, Ontario, Canada. The test started in July 2022 and is scheduled to be completed in September 2023.

Figure 1: Test article and test setup

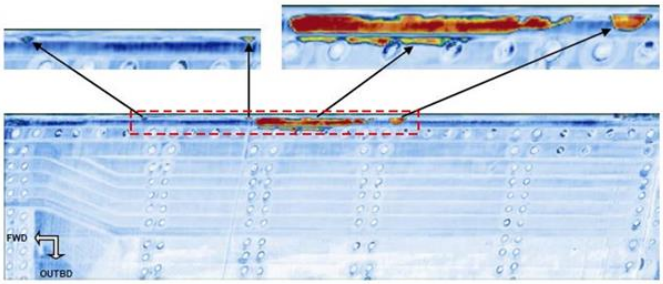

Figure 2: Disbond on test article lower step lap joint

2.1.4 REFERENCES

[1] Dionne, E, Backman, D., Beltempo, A., Brunet, S., and Bolduc, B., Experimental Strength and Fatigue Assessment of a Disbonded F/A-18A/B/C/D Inner Wing Step Lap Joint, Proceedings of the 31st Symposium of the International Committee on Aeronautical Fatigue and Structural Integrity (ICAF2023), 26 – 29 June 2023, Delft, The Netherlands.

2.2 Bell 525 Relentless Aft Fuselage / Tailboom and Aft Tailboom / Vertical Fin Certification Testing *

Andre Beltempo, NRC Aerospace

* Full paper being presented at ICAF2023

Since 2019, the National Research Council of Canada (NRC) has been conducting certification fatigue testing of the vertical fin, aft fuselage, and tail boom of the Bell 525, a super medium commercial transport helicopter under development by Bell Textron. Specialized test methods, data collection and analysis are used for these composite/metallic hybrid structures. The approach for testing these full-scale components was developed in partnership with the National Research Council Canada (NRC). Testing for initial structural certification was completed at the Structural Integrity Lab M-14 in Ottawa, Canada. Some of these details are available in a paper presented at ICAF2023 [2].

Two test articles are being tested, 1) the aft fuselage and tailboom; 2) the aft tailboom and vertical fin. The empennage structures under consideration are located downstream of the turbine engine exhaust and are thus subject to high temperature (hot/wet) operating conditions. To validate the hybrid structure while accounting for the impact of a hot/dry environment on composites, the test articles were encased in custom NRC designed heated enclosures, shown in Figure 3 and Figure 4. The use of heated enclosures allowed a significant reduction in the required environmental load factor, with the remaining difference between a hot/dry and hot/wet condition requiring only a small load correction. As a result, the test loads permitted both the composite and metallic structures to be appropriately evaluated simultaneously.

Both test articles successfully completed a comprehensive durability and damage tolerance test campaign, where the tested structural components incorporated embedded flaws and impact damage. Testing included repeated residual strength testing and additional load cycling in the presence of additional larger structural impact damage. Successful completion of these tests demonstrated the validity of the approach and provided Bell with sufficient information to show compliance for FAA certification.

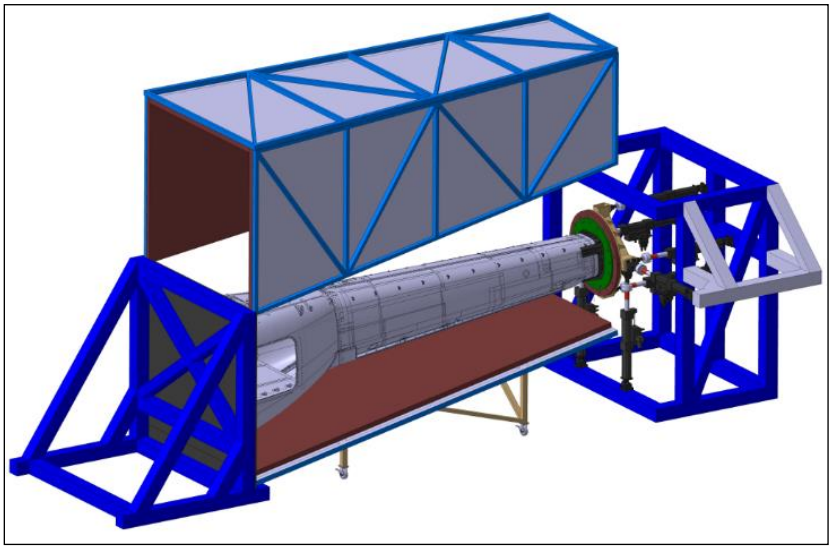

Figure 3: Aft fuselage / tailboom test rig showing heated enclosure

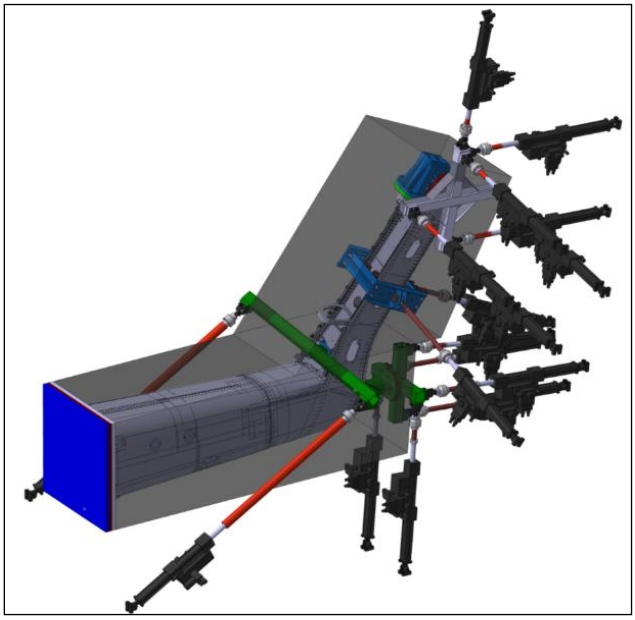

Figure 4: Vertical fin test rig showing heated area in grey

2.2.1 REFERENCES

[2] Beltempo, C.A., Langlois, P, Colle, A.R., and Rogers, J., Bell 525 Relentless Aft Fuselage / Tailboom and Aft Tailboom / Vertical Fin Certification Testing, Proceedings of the 31st Symposium of the International Committee on Aeronautical Fatigue and Structural Integrity (ICAF2023), 26 – 29 June 2023, Delft, The Netherlands.

3.0 AIRCRAFT STRUCTURAL INTEGRITY PROGRAM AND FLEET MANAGEMENT

3.1 CF-188 Aircraft Structural Integrity Program (ASIP) and Aircraft Life Extension (ALEX) Program

L3Harris - Military Aircraft Services (MAS)

L3Harris MAS, a wholly owned subsidiary of L3Harris, is among Canada's leading In-Service Support (ISS) integrator, offering military and commercial customers a full range of modifications and sustainment solutions, in support of their aircraft fleets. L3 MAS employs over a thousand people in its main facility in Mirabel, Quebec and in other operating centers throughout Canada (Bagotville, Cold Lake, Halifax, Shearwater, Comox, Pat Bay, Greenwood, Gatineau, Ottawa, Toronto, Trenton and Petawawa). L3Harris MAS provides ISS services to the Royal Canadian Air Force (RCAF) on the following platforms:

- CF-188 Hornet
- CT-114 Tutor
- CH-148 Cyclone
- CC-150 Polaris
- CP-140 Aurora

Since 1986, L3Harris MAS performs the in-service support of the Royal Canadian Air Forces (RCAF) CF-188 Hornet (Boeing F/A-18) fleet as part of System Engineering Support Contract (SESC). This contract includes the conduct of all aspects of the Aircraft Structural Integrity Program (ASIP) and of related depot level structural maintenance.

In 2022, MAS was awarded a new Sustainment Performance Based Contract (PBC) on the CF-188 to support the last 10 years of service. The framework of this contract increases the responsibility/authority of L3H MAS with fleet management and airworthiness activities. In order to meet the contractual key performance indices, MAS must manage and guarantee to a minimum number of aircraft available to the RCAF at all time and to respond to parts query in a short timeframe. This PBC also aims at reducing costs via fleet management and usage management efforts.

In parallel to this new PBC, MAS is finalising the introduction of the Interim Fighter Capability Program (IFCP), which represents 13 jets converted from the RAAF to complement the legacy fleet until the introduction of the Future Fighter Capability Program (FFCP) as early as 2025.

MAS was also mandated by the RCAF to develop and implement the Hornet Extension Program (HEP), a series of upgrades to the CF-188 avionics and armament capabilities. This program is entering its full-rate production phase as of summer 2023.

3.1.1 FLIGHT CONTROL SURFACES LIFE EXTENSION

As previously reported in previous ICAF cycles, the extension of the life of the Flight Control Surfaces (FCS) is one of the last major efforts required to support the extension of the Expanded Life Expectancy (ELE) of 2032. The certification strategy is primarily based on full-scale component testing of the Horizontal Stabilator, aileron, inboard leading edge flap and trailing edge flap. MAS and the NRC, the test agency, have been working in close collaboration on these programs. These tests were all completed prior to this reporting cycle; however, further details are provided below for the Horizontal Stabilator and the Trailing Edge Flap where the in-service management presents a greater challenge.

3.1.2 TRAILING EDGE FLAP TESTS (TEF)

The Trailing Edge Flap (TEF) attach hinges do not meet the ELE target of 7,000 Component Flight Hours (CFH). Due to the urgency of certifying the outboard hinge, it was decided to set up a dedicated test for that purpose alone. The outboard hinges have been replaced and have two hot spots that have been subjected to modifications shortly after the replacement. Results of this test has only allowed a moderate extension of the life of the hinge and some hinges will fall short of the 7,000 CFH target if they were replaced and/or were modified too early. The situation is currently being assessed at the asset management level to see if component swaps will be sufficient to meet the ELE.

The inboard hinge also has two known hot spots, one of which was found cracked in-service (lug bore). The short-term strategy to bridge the gap to 7,000 is expected to be a Safety by Inspection (SBI) program around 6000-6500 hours for the lug bore and an Aircraft Sampling Inspection (ASI) for the horizontal flange (analytical hot spot). The medium-term strategy is to refine the lifing of this hinge via an on-going component test at NRC (FTS4), which is mainly funded by the Swiss Air Force. Results are expected by the end of 2023.

3.1.3 HORIZONTAL STABILATOR

The RCAF fleet has two Horizontal Stabilator (H-Stab) configurations; the older with some areas fabricated with 2.3 pcf (pounds by cubic foot) aluminum honeycomb core and the second, including the majority, with 3.1 pcf instead. Effort was undertaken to extend the 2.3 pcf configuration but radiographic inspection revealed severe core deformations, which may be attributed to fatigue at some areas subject to high deformations and dynamic loading. On the other hand, for the 3.1 pcf, a fatigue test (i.e., FT905) was performed at NRC on a retired USN H-Stab with more than 6000 CFH that was subjected to aggressive environmental conditions. During the

test, the article sustained 41000 Simulated Flight Hours (SFH) for durability testing, and, following damage introduction, another 11000 SFH for damage tolerance testing. For the Residual Strength Test (RST), 120% of Design Limit Load (DLL) multiplied by an Environmental Factor (EF) was applied. Finally, a variety of inspections (X-Ray, C-Scan, pulse flash thermography) were performed including a destructive teardown and no growth of any kind of damage was observed with no evidence of core fatigue. Therefore, by inspecting these H-Stab at 7000 CFH, it is possible to safely extend their service life up to 10000 CFH ((10000 SFH + 40000 SFH) / 5). However, while performing full X-Ray inspection on in-service H-Stabs, many damages or defects were identified such as adhesive cracks, partial skin to core adhesive separations and deformation of the core. Even if these discrepancies are somewhat common, there is no systematic basis to accept them because they can be fatigue related. Therefore, a closer review of FT905 X-Ray (Pre & Post-test) was carried out to identify any discrepancies to clear by comparison with the damages found. Since then, it is possible to clear many findings on the 3.1 pcf without additional actions.

3.1.4 OUTER WING MAINTENANCE INDUCED DAMAGE (MID) TEST

MID has been reported on both the RAAF and RCAF FA-18 fleets at the Lower and Upper surfaces of the outer wing forward spar at the root of the Outboard Leading Edge Flap (OLEF) transmission attach lugs. These appear to have been induced by sharp instruments used to cut the sealant above these lugs under the seals, likely from in-service maintenance (see Figure 5). The MID location also coincides with the peak stress location on these lugs (see Figure 6). This led to the nucleation and apparently fast propagation of cracks severing several lugs before they were caught.

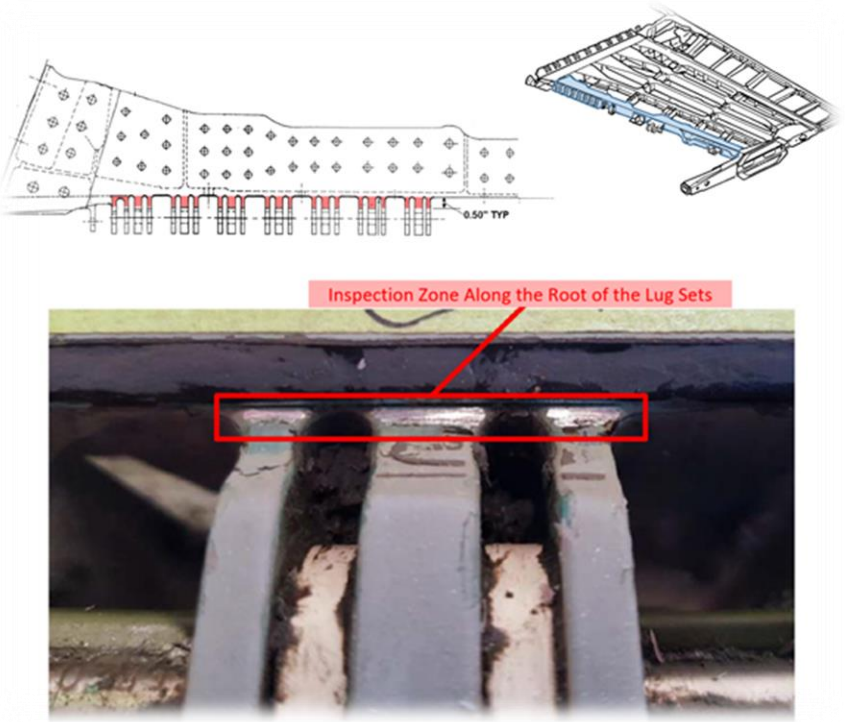

Figure 5: OW forward spar MID location

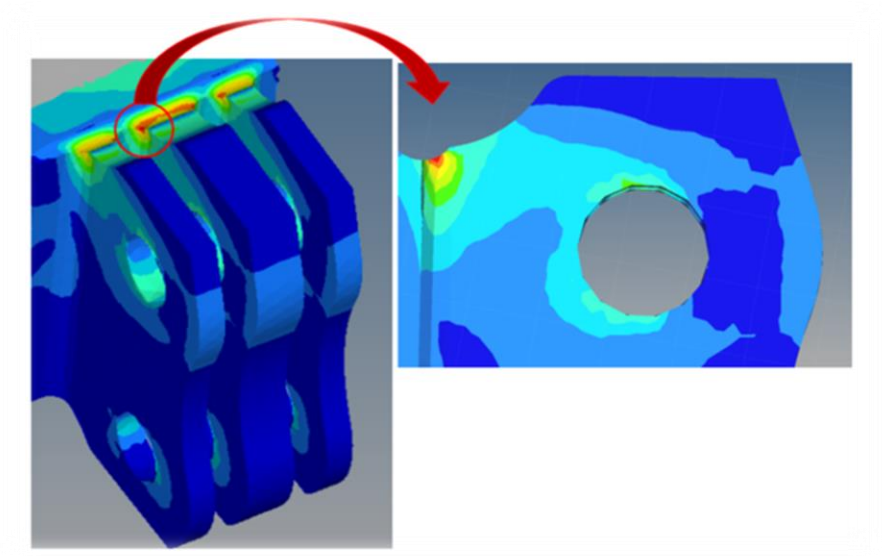

Figure 6: OW forward spar peak stress location

The repair concept (originally developed by the RAAF) was not considered full life and was only substantiated analytically in crack growth, leading to fairly small post repair inspection intervals (see Figure 7). Since the RCAF is expecting to fly their outer wings longer than the RAAF, a longer post-repair life was desired by also accounting for the new post-mod CI (crack initiation) life generated by the repair blend. In addition, to repair deep damage, a revised deeper repair scenario was developed using a wider blend radius. This deeper blend will be accomplished using a numerical controlled milling fixture.

Figure 7: Light repair blend

The certification of the light blend repair version (covering the majority of wings) has been covered by component testing at NRC, Ottawa under FT390. The deeper blend was therefore "pegged" on the test results using ratio of stresses from FEA.

The test article includes an Outboard Leading Edge Flap mounted on an OW with four jacks applying manoeuvre loads. After a loads influence review, it was found that wing bending loads had negligible influence so only OLEF loads were applied. Then the lugs were instrumented adjacent to the blend area (see Figure 8). The test is now completed and allowed to substantially increase the initial preliminary post mod life (from 227 to 1164 HRS for the light blend and from 946 to 1684 hrs for the deeper blend).

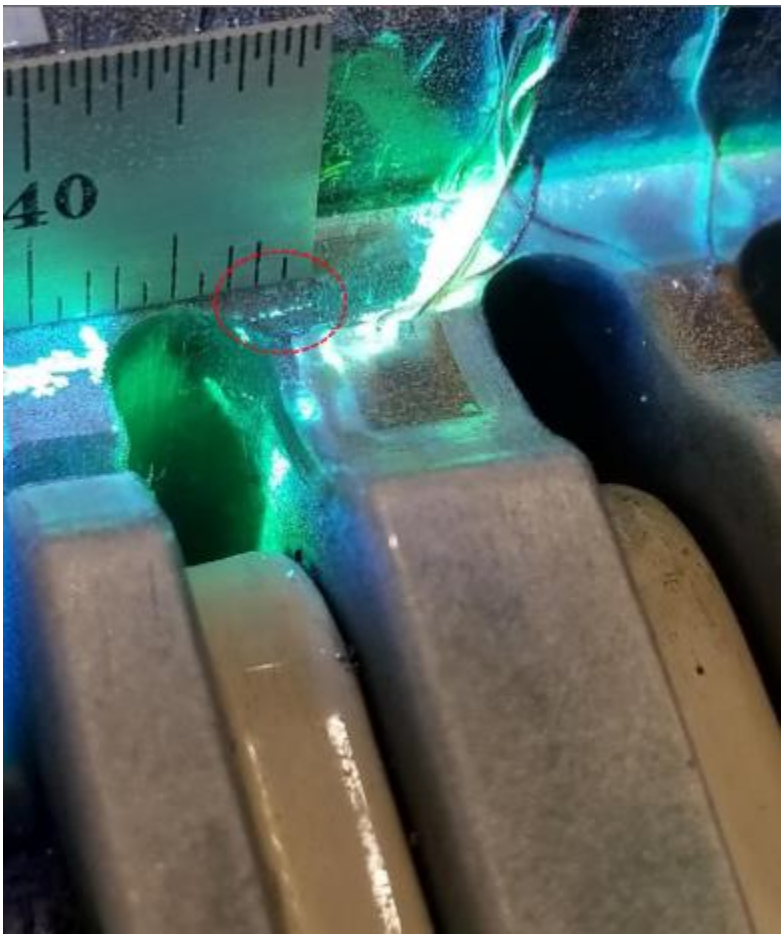

Figure 8 Strain gauge location

3.1.5 H-STAB SPINDLE BUSHING WEAR REPAIR

As part of the periodic inspection program every 600 airframe hours, the horizontal stabilator bushings are inspected for wear as only a small deviation in the gap between the bushing and bearing could potentially induce severe flutter (see Figure 9). A few years ago, a few aircraft were

reported with gaps above the maximum allowable gap of 0.0055'', which led to a bushing replacement. Such repair is a costly endeavour as it requires a fly-in to depot, remove the spindle fitting from the aircraft, machine it down carefully to remove it, heating the new bushing to ease its installation, and finally machine down the bushing outside diameter to the final specifications of the Original Equipment Manufacturer (OEM). This activity also led to the finding of collateral damages on the aircraft mating surfaces.

More recently, it was found that the measuring technique was deficient on a few aircraft so a measuring jig was developed to provide more accurate dimensions. This jig replicates the spindle geometry and stiffness with a new bearing installed (see Figure 10). In any case, the natural ageing of the aircraft shows that gaps on many planes are getting very close to the maximum allowance.

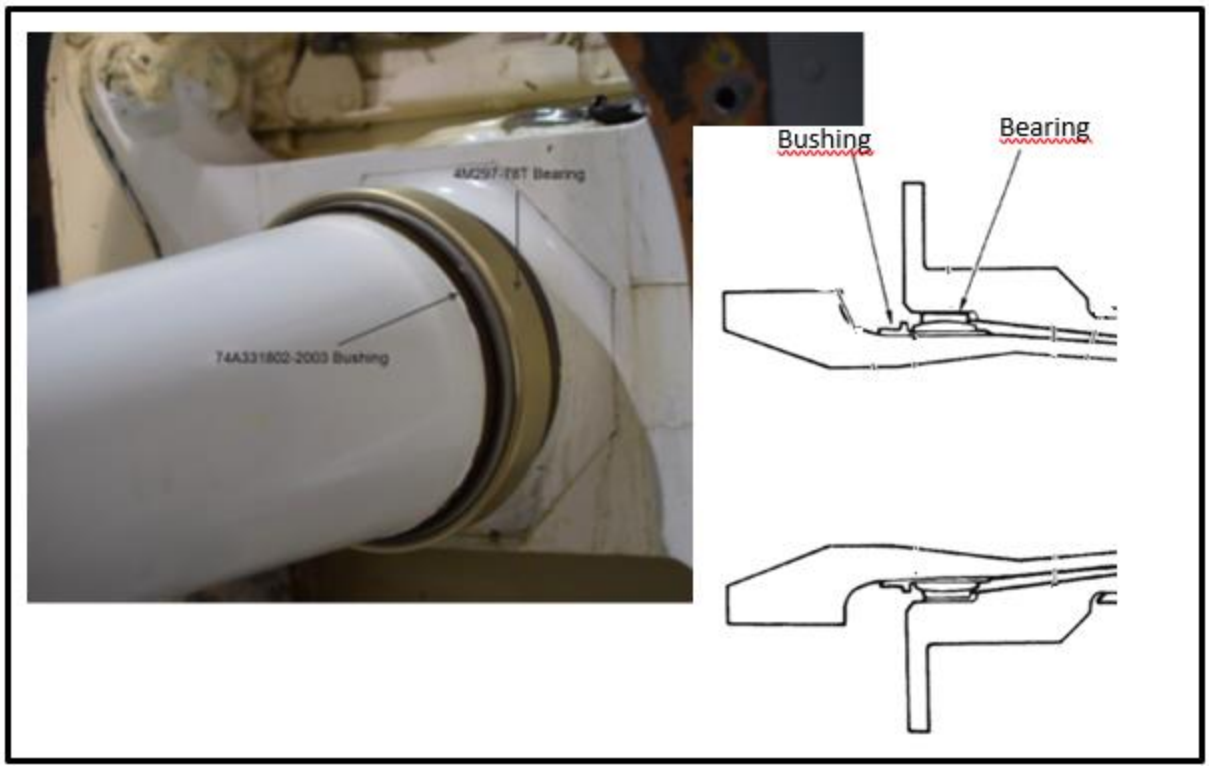

Figure 9: H-Stab spindle bushing

Figure 10: Spindle bushing measuring jig

To address this degrading situation, various other options are being considered to reduce the repair cost and downtime associated to an excessive gap:

1) Increase the wear limit via a Ground Vibration Test (GVT)
    - Likely need only to show 0.001” or 0.002’’ increase gap but GVT is relatively expensive
    - A detailed plan was prepared and the solution deemed viable, if ever needed
2) Cadmium plating: A repair consisting of rebuilding the gap (several thousands of an inch) with cadmium plating was successfully tested (Figure 11).
    - What remains to be demonstrated is the cadmium plating wear durability
    - The intent would be to measure repaired gaps more often to collect data and then increase inspection interval back to the current practice when sufficient confidence is gained
3) Manufacture a new bearing with smaller inside diameter to reduce the gap (would need to evaluate practical aspects first with respect to H-Stab installation.)

At this point, the plan is to use Option 2 at the next occasion.

Figure 11: Bushing material build up repair with cadmium plating

3.2 CT-114 Tutor Aircraft Structural Integrity Program (ASIP)

L3Harris - Military Aircraft Services (MAS)

Aircraft usage monitoring is achieved by collecting, evaluating and processing the Operational Loads Monitoring (OLM) system data. Periodically, collected aircraft usage data is validated and accumulated fatigue damage is calculated for major aircraft components. In addition, remaining life for every major aircraft component is calculated based on the predicted aircraft usage by the General Integrated Fatigue Tracking Software (GIFTS) module of the Tutor Engineering Database (TED) system. The monitoring program findings and L3 MAS recommendations are reported to the Department of National Defence (DND) on a monthly basis.

Aircraft condition monitoring is carried out by reviewing damage and repair reports and inspection results to identify trends and assess the long-term impact at or near critical locations and other repairs. Structural Significant Items (SSI) are monitored and corrective actions are identified such as modifications, standard repairs, or amendments to the inspection and maintenance program. Findings and recommendations are reported to DND via several reports, including the Corrosion Prevention Control Plan (CPCP), Durability & Damage Tolerance Control Plan (DDTCP), Structural Maintenance Plan (SMP), Aircraft Structural Integrity Management Plan (ASIMP).

MAS was mandated to extend the service life of the Tutor fleet to 2030. An ageing aircraft program is being developed to review structural records related to the structure, avionic, electrical and mechanical systems. A general condition survey will provide additional data and an assessment of additional inspections required to bring the Expanded Life Expectancy (ELE) to 2030 will be made. In parallel, an obsolescence management plan was created to prevent and resolve component

and stock procurement issues. An avionic upgrade is also currently ongoing to comply with the regulation until 2030. A staggering tool is being developed to create and update a fleet strategy to manage the rotation of service aircraft with those in storage in order to meet the new planned retirement date.

Figure 12 CT-114 Tutor (Snowbird, [http://www.canadianflight.org/content/canadair-ct-114-tutor)](http://www.canadianflight.org/content/canadair-ct-114-tutor)

3.3 CH-148 Maritime Helicopter Aircraft Structural Integrity Program (ASIP)

L3Harris - Military Aircraft Services (MAS)

As part of the Maritime Helicopter Program, L3 Harris MAS is mandated to conduct an ASIP program on the S-92, designated as CH-148 by the Royal Canadian Air Force (RCAF). Usage monitoring is performed using raw data files collected through the Health and Usage Monitoring System (HUMS). The HUMS has the capability to recognize regimes/manoeuvres via recorded flight parameters and sensor data. This data is processed by the Usage Comparison and Reporting Tool (UCART) that computes fatigue damage rates at selected locations for each individual aircraft and compares them to the design spectrum according to the requirements of MIL-STD-1530.

Since 2021, several algorithms for fatigue damage rate derivation in UCART from the HUMS regime and event data have been corrected for improved accuracy. The control points forecasted at the early days of the program have been changed and some others have been added. Filtering of the captured regime data was implemented in order to provide realistic usage data and avoid multiple triggering of the regime recognition when aircraft is operating close to the defined thresholds. Additional modifications were also made to UCART to correct false ship-based taxi signal discovered during Regime recognition validation.

The other major component of the CH-148 ASIP Program is the Structurally Significant Item (SSI) database. The SSI database records all the relevant information about each SSI, also known as Primary Structural Element (PSE), from the design phase and into the in-service phase in order to enable ASIP analysts to monitor structural defects and, when needed, recommend changes to the maintenance program or modifications to the helicopter.

Usage monitoring and structural condition monitoring are now well implemented and periodic reporting is now done, in support of the fleet management.

Figure 13 CH-148 Cyclone helicopter (https://en.wikipedia.org/wiki/Sikorsky_CH-148_Cyclone#/media/File:Canadian_CH-148_Departs_Flight_Deck_During_Keen_Sword_21_(cropped).jpg)

3.4 CC-150 Polaris Fleet In-Service Support and Fleet Management

L3Harris - Military Aircraft Services (MAS)

As part of the Polaris Program, L3 Harris MAS Inc is mandated to provide in-service support for the operations of the five CC-150 Polaris aircraft (Airbus A310-304) of the Department of National Defence (DND). L3 MAS develops and maintains an A310 maintenance schedules to satisfy 180 minutes of Extended range Twin-engine Operations (ETOPS) and CC-150 specific modifications. MAS also provides engineering support to satisfy Canadian Forces operational requirements and the configuration control of the CC-150 Polaris (A310 Airbus) fleet, as well as Reliability monitoring based on Airworthiness Manual Advisory AMA 571.101/1 to monitor the effectiveness of the CC-150 maintenance program.

L3 MAS also provides System engineering and Airworthiness support to satisfy Canadian Forces operational requirements and the configuration control of the CC-150 Polaris (A310 Airbus) fleet. As part a Polaris Program Contract Amendment, L3 MAS is also mandated to provide In-Service Support services for two used A330 aircraft operated as VVIP and Passenger transport aircraft of the Department of National Defence (DND). The period of performance is from December 2022 to December 2024, with an option to extend up to two additional years.

Figure 14 CC-150 Polaris in tanker configuration https://en.wikipedia.org/wiki/Airbus_CC-150_Polaris#/media/File:RCAF_CC-150_Polaris_Davies.jpg)

3.5 Development and Demonstration of Damage Tolerance Airframe Digital Twin Methods and Tools*

Yan Bombardier, Guillaume Renaud, and Min Liao, NRC Aerospace
* Full paper being presented at ICAF2023

The National Research Council of Canada (NRC) has been developing an airframe digital twin (ADT) framework and tools to support structural life-cycle management for the Canadian Department of National Defence (DND) [3][4]. The primary objective of NRC's ADT framework is to enhance the accuracy of structural diagnosis and prognosis to facilitate better maintenance decisions. This ADT framework integrates cutting-edge structural analysis, probabilistic modelling techniques including: advanced probabilistic crack growth modelling, high-fidelity finite element simulations, and quantitative risk assessment. The framework also provides the capability to periodically update the probabilistic inputs of these models as new data, such as inspection results, usage, and other relevant factors about the airframe, become available.

The risk-based approach, used in NRC's ADT framework, provides tools and methods to relax some of the conservative assumptions imposed by the damage tolerance approach. Consequently, the adoption of the ADT framework proposed and developed by NRC requires a change in how aircraft are currently lifed; moving from conservative deterministic approaches to quantitative risk assessment approaches.

Recent improvements incorporated into the ADT framework expanded its capability to real-world applications, allowing users to:

- Maintain an aircraft using a risk-based approach. Risk can be quantified in terms of single flight-hour probability of failure (SFHPOF) / hazard rate, or cumulative probability of failure.
- Perform tail-specific analyses based on available data, including inspection results and load monitoring.
- Update prior engineering assumptions based on data collected throughout the life of the aircraft. This includes loads and the initial crack size distribution (ICSD) that have significant effect of the SFHPOF.
- Intrinsically include uncertainty quantification, such that the known unknowns are modelled and can affect the calculated life distribution. This approach theoretically replaces legacy engineering approaches that rely on safety factors.
- Adjust the complexity of the analyses based on available information. At a minimum, the ICSD and the probability of detection (POD) curve should be provided. However, it was shown that the work performed by other organizations and engineering judgement can be leveraged to estimate these parameters. While more representative values should yield to more reliable results, conservative assumptions can also be used provided that the inference capability of the framework could help to refine these assumptions throughout the life of the aircraft.

The ADT framework was demonstrated with the CF-188 ILEF attachment lugs shown in Figure 15. This provided an excellent opportunity to develop and test the new concepts. However, it was found that the CF-188 ILEF case study might not be well suited for the damage tolerance approach. The use of mixture distributions for modelling the ICSD has been investigated for this case study [3]. While this modelling method requires additional data in the form of ICSD for various types of defects, it was shown that these data can be obtained from the literature and measurements to develop more physics-based ICSD supported by tests and in-service data.

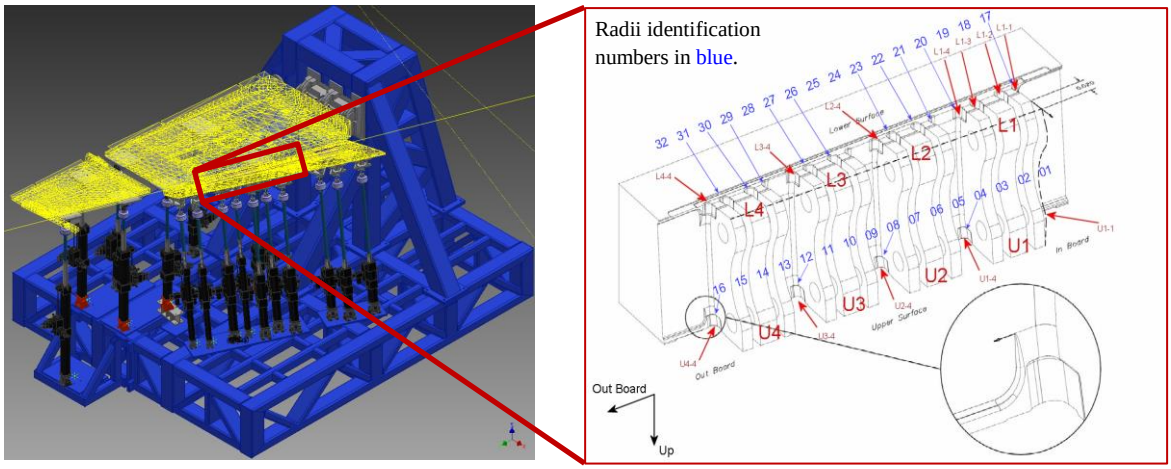

Figure 15: ILEF areas of interest

Two inference methods that use non-destructive inspection (NDI) results were also investigated using CF-188 ILEF case study. The first method is used to infer the crack size distribution describing the damage state in the structure. The second method is used to infer the mixture weight distribution of the constituting crack size distributions representing various types of damage that could be present in the structure. This assessment showed that only the crack size distribution inference approach could sufficiently decrease the SFHPOF to allow safety by periodic inspections. However, it is recommended to investigate the mixture weight inference method further before drawing strong conclusions on its relevance for lifing and sustainment of airframe structures [3].

3.5.1 REFERENCES

[3] Bombardier, Y., Renaud, G., Liao, M., Development and Demonstration of Damage Tolerance Airframe Digital Twin Methods and Tools, Proceedings of the 31st Symposium of the International Committee on Aeronautical Fatigue and Structural Integrity (ICAF2023), 26 – 29 June 2023, Delft, The Netherlands.

[4] Liao, M., Renaud, G. and Bombardier, Y. (2023) Digital twin technology development and demonstration for aircraft structural life-cycle management. In NDE 4.0, Predictive Maintenance, Communication, and Energy Systems: The Digital Transformation of NDE (Vol. 12489, pp. 16-26). SPIE.

4.0 FATIGUE LIFE ASSESSMENT AND ENHANCEMENT TECHNOLOGIES

4.1 Fatigue Life Prediction of Metallic Materials using Tanaka-Mura-Wu Model *

S. Li[1], X.J. Wu[2], R. Liu[1], and Z. Zhang[2]
[1]Carleton University, Department of Mechanical and Aerospace Engineering, Canada
[2]National Research Council Canada, Canada
* Full paper being presented at ICAF2023

As fatigue failure continues to be a threat to the structural integrity of engineering platforms such as aircraft, accurate and efficient fatigue life prediction methods are needed in their design, certification and maintenance. Traditionally, a large amount of fatigue testing has to be performed to determine the fatigue properties of a material and establish the correlation between fatigue life and loading parameters, such as the Coffin-Manson-Basquin equation. However, this exercise is very costly and prolongs the product development cycle.

The Aeronautical Product Development and Certification (APDC) Program is setup at the National Research Council of Canada (NRC) to develop methods of certification by analysis (CbA), aiming at supporting the industry to achieve high-efficiency and low-cost product development. First, NRC has developed a dislocation-based fatigue crack nucleation model—the Tanaka-Mura-Wu (TMW) model, by modifying the original Tanaka-Mura model, which evaluates fatigue crack nucleation life by elastic modulus, Poisson's ratio, surface energy and the Burger's vector. The TMW model application to fatigue life prediction was studied for different engineering materials such as aluminium alloys, titanium alloys, nickel-based superalloys, low-carbon steels and alloy steels. Comparisons with the Coffin Manson Basquin relations were made to validate the model. It was shown that the TMW model is able to provide class-A prediction (forecast prior to the event) over the full fatigue range including low cycle fatigue (LCF) and high cycle fatigue (HCF), without resorting to fatigue testing and calibration (Figure 16). The model establishes a physics-based baseline for characterizing the effects of other influential factors including microstructure and surface roughness on the fatigue life of a material, which contributes to scattering in fatigue properties.

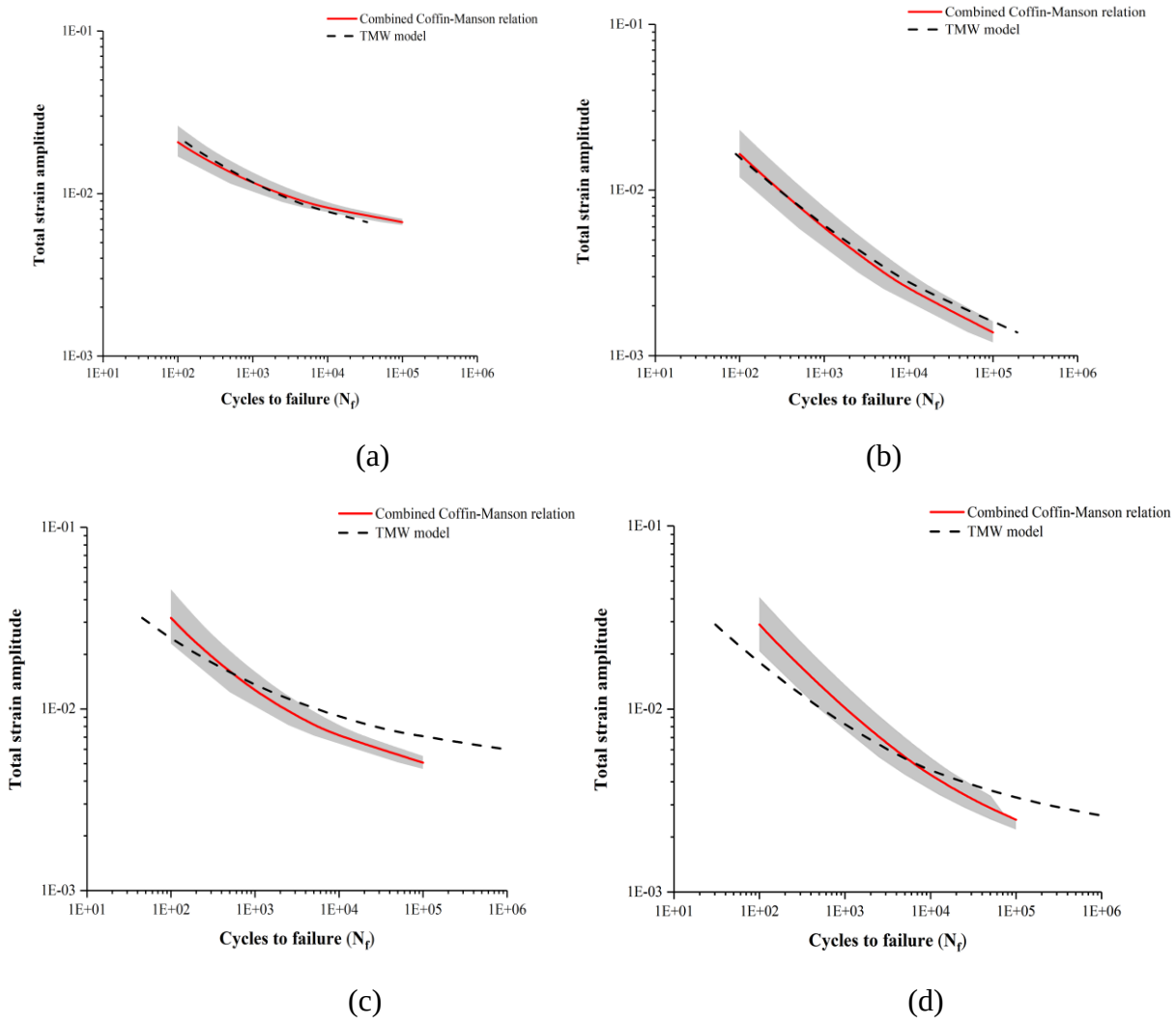

Figure 16: Comparison between the TMW model and CMB relation for a) 7075-T6, b) SAE 1020, c) Ti6Al4V, and d) IN617

4.1.1 REFERENCES

[5] Li, S., Wu, X., Liu, R., and Zhang, Z., "Full-Range Fatigue Life Prediction of Metallic Materials Using Tanaka-Mura-Wu Model," SAE Int. J. Mater. Manuf. 15(2):2022, doi:10.4271/05-15-02-0010.

[6] Li, S., Wu, X., Liu, R., and Zhang, Z., "Full-Range Fatigue Life Prediction of Metallic Materials Using Tanaka-Mura-Wu Model", Proceedings of the 31st Symposium of the International Committee on Aeronautical Fatigue and Structural Integrity (ICAF2023), 26 – 29 June 2023, Delft, The Netherlands.

4.2 Probabilistic Lifing of a Second Oversize Hole Modification

Guillaume Renaud*, Éric Dionne, and Min Liao, NRC Aerospace
* Full paper being presented at ICAF2023

Hole oversizing is a common technique used to remove potential or existing cracks in fastener holes. When used as a fleet-wide modification, hole oversizing is often preceded by non-destructive inspection that does not necessarily report damage. Depending on the crack detection capability and the level of oversizing, undetected cracks may not be completely removed by the modification. The approach currently used by the Royal Canadian Air Force for lifing the CF-188 second oversized holes is to assume that an undetected residual crack is always present at the hole after the modification. This approach may be overly conservative, especially in a safe life analysis context.

A probabilistic methodology was proposed by L3Harris to reduce conservatism by estimating the post-modification damage state from the pre-modification crack size distribution, determined from the CF-188 lifing methodology. This methodology was shown to be useful when implemented fleet-wide to reduce maintenance costs while maintaining an acceptable probability of failure. The National Research Council of Canada (NRC) assessed this methodology and enhanced it to better characterise the probability of detection and its effect on the residual cracks, and to add the ability to apply the method tail-by-tail [7]. These enhancements were demonstrated on a second oversize hole modification performed on the CF-188, as seen in Figure 17. It is believed that the developed methodology could be useful for increasing the safe life limit of locations that are short of their target life, especially for ageing fleets.

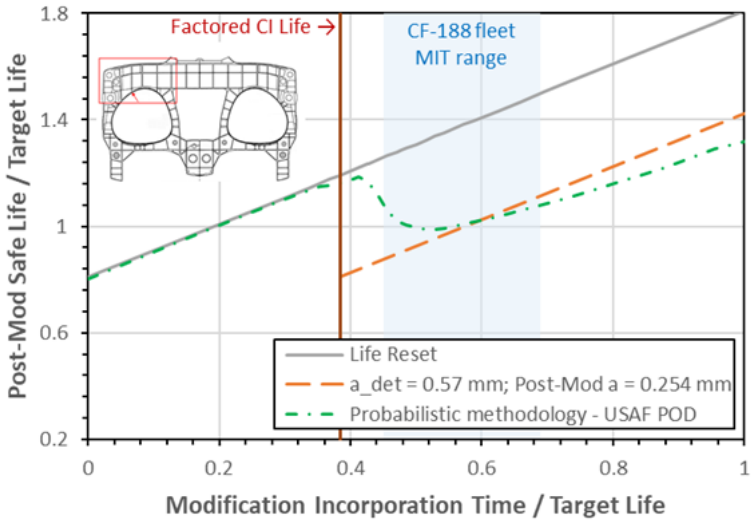

Figure 17: Probabilistic methodology results for ALEX 6.0 modification

4.2.1 REFERENCES

[7] Renaud, G., Dionne, E and Liao, M (2023), "Probabilistic Lifing of a Second Oversize Hole Modification", Proceedings of the 31st Symposium of the International Committee on Aeronautical Fatigue and Structural Integrity (ICAF2023), 26 – 29 June 2023, Delft, The Netherlands.

4.3 Investigation of the Tensile/Compressive Residual Stresses in AISI4340 Steel under Low-Cycle Fatigue Loading *

M.A. Patrick, J.F. Laliberté, X. Wang, Carleton University
* Full paper being presented at ICAF2023

This work builds on existing literature to study the low-cycle fatigue properties of notched components under various loading conditions for application to landing gear fuse pins [8]. A primary consideration in the fatigue life prediction of fuse pins is the complex stress state surrounding the inner circumferential notch. Accurate fatigue life prediction of these components is challenging due to the component geometry and unpredictable loading histories, such as overloads induced by hard landing events. This research investigates the effects of complex residual stresses induced by a single initial overload on the low-cycle fatigue life of notched AISI 4340 steel specimens. Additionally, a design assumption used in industry of equating the maximum residual stress at the notch root to a mean stress is investigated.

The experimental test setup is shown in Figure 18. Control specimens were subjected to quasi-static low-cycle fatigue using the strain-life model. Variable specimens were subjected to either a quasi-static initial overload prior to fully reversed low-cycle fatigue loading, or a mean stress of identical magnitude as the residual stress induced from the applied overload. The magnitude of the residual stress at the notch root was determined using elastic-plastic FEA in ABAQUS-2021x, as shown in Figure 19 for a compressive overload.

The tensile residual stress induced through compressive overload caused a 23% decrease in fatigue life, while the compressive residual stress induced by tensile overload caused a 5% increase in fatigue life. Strain life mean stress correction models, namely the Smith-Watson-Topper (SWT) and Morrow mean stress correction models, both provided nonconservative estimates for life predictions compared to experimental data, however the SWT model was more accurate. Predictive results were highly dependent on fatigue ductility exponent *c* in the low-cycle fatigue regime. It was also shown that the applicability of strain-life methodologies is suitable for specimens having undergone load-controlled testing. These results are significant in the design of components where plasticity must be considered in fatigue life assessments.

Figure 18: Experimental setup of notched AISI 4340 fatigue coupons

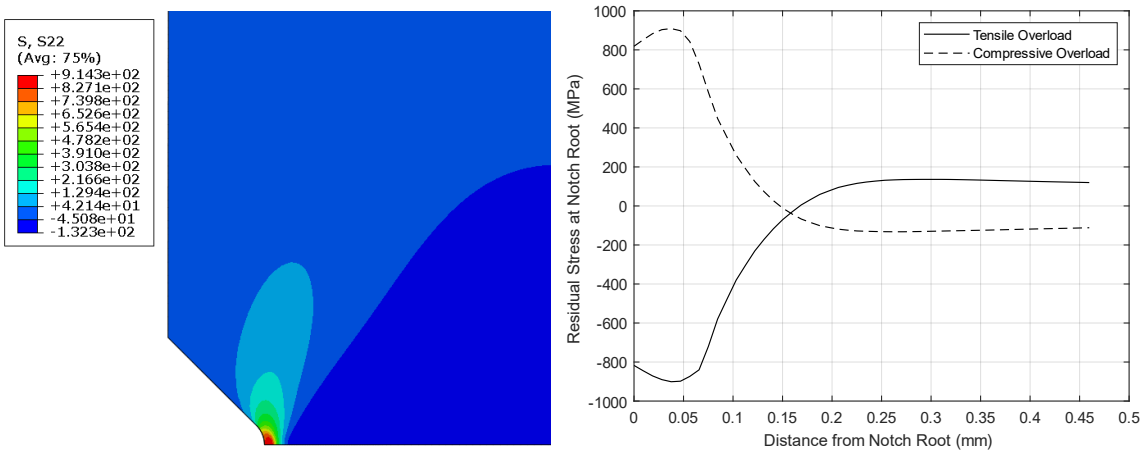

Figure 19: Residual stress due to an ±11 kN overload relative to distance from notch root

Through investigating the residual stress – mean stress design assumption, equating the tensile residual stress as a positive mean stress caused a reduction in estimated fatigue life to provide a conservative life estimate. However, equating the compressive residual stress to a negative mean stress for fatigue life predictions provided a highly non-conservative estimate. Additionally, fractographic results demonstrated that the effects of single initial overloads influenced only the crack initiation region, while mean stresses had a significant effect on the size of the crack propagation region. These fractographic differences further denounce the usage of the design assumption equating a residual stress to a mean stress. Evaluation of the applicability of the residual stress to mean stress approximation is critical in ensuring conservative estimates are used in engineering applications.

4.3.1 REFERENCE

[8] C. Bassindale, R. E. Miller, and X. Wang, "Effect of single initial overload and mean load on the low-cycle fatigue life of normalized 300 M alloy steel", International Journal of Fatigue, 130 (2020), 105273.

[9] M.A. Patrick, J.F. Laliberté, X. Wang, Investigation of the Tensile/compressive Residual Stresses in Aisi 4340 Steel Under Low-cycle Fatigue Loading, Proceedings of the 31st Symposium of the International Committee on Aeronautical Fatigue and Structural Integrity (ICAF2023), 26 – 29 June 2023, Delft, The Netherlands.

4.4 Pipeline Condition Monitoring Towards Digital Twin Ecosystem: A Case Study

Teng Wang and Zheng Liu, UBC Intelligent Sensing, Diagnostics, and Prognostics Research Lab

Pipeline conditional monitoring is usually driven by the entity in its physical space, with little connection to its virtual space. However, with the advancement in digital twin (DT) technology, it is possible to implement the seamless convergence of physical and virtual space. Supported by the Canada-Germany 3+2 Joint Program, the University of British Columbia (UBC) Intelligent Sensing, Diagnostics, and Prognostics Research Lab (ISDPRL) is currently investigating the pipeline condition monitoring towards the DT ecosystem in collaboration with the NRC (National Research Council of Canada), IKTS (Fraunhofer Institute for Ceramic Technologies and Systems), and two industrial partners from Canada and Germany, respectively.

Based on previous work [10], the pipeline DT ecosystem is shown in Figure 20. In this framework, the pipeline DT is built based on the individual physical pipeline and pipeline knowledge library. Bayesian inference online updates the pipeline DT according to real-world findings from the individual physical pipeline. The pipeline knowledge library provides the initial assumption, prior knowledge, best-available models, and future operational condition to support the running of the ecosystem. The operators can interact with DT from the service station and be informed of the condition of the pipeline for maintenance decision-making.

To prototype a DT ecosystem for pipeline condition monitoring, a case study is conducted based on some pipe fatigue tests, as shown in Figure 21. Specifically, a set of pipes under cyclic loading are considered in this study [11]. The cyclic loading is simulated from the four-point bending machine. In real-world applications, cyclic loading is generally caused by the pressure variation of the pipeline. Due to the cyclic loading, it is expected that a circumferential crack will arise in the welded joint and grow along the weld. In this case study, the guided-wave sensor network is deployed to acquire the damage sensory data. In particular, the measurement accuracy (MA) and probability of detection (POD) of the sensor network are quantified. The probabilistic model is designed to quantify the randomness of the operational loading conditions. Finite element (FE)

analysis is conducted to calculate the stress intensity factors at the crack tips. To achieve computational efficiency, a data-driven model is built as the surrogate of the FE solutions. Bayesian inference is adopted to update the crack location and length prediction results according to the sensor network readings. Moreover, the augmented reality technique is employed to visualize the virtual model and the prediction result.

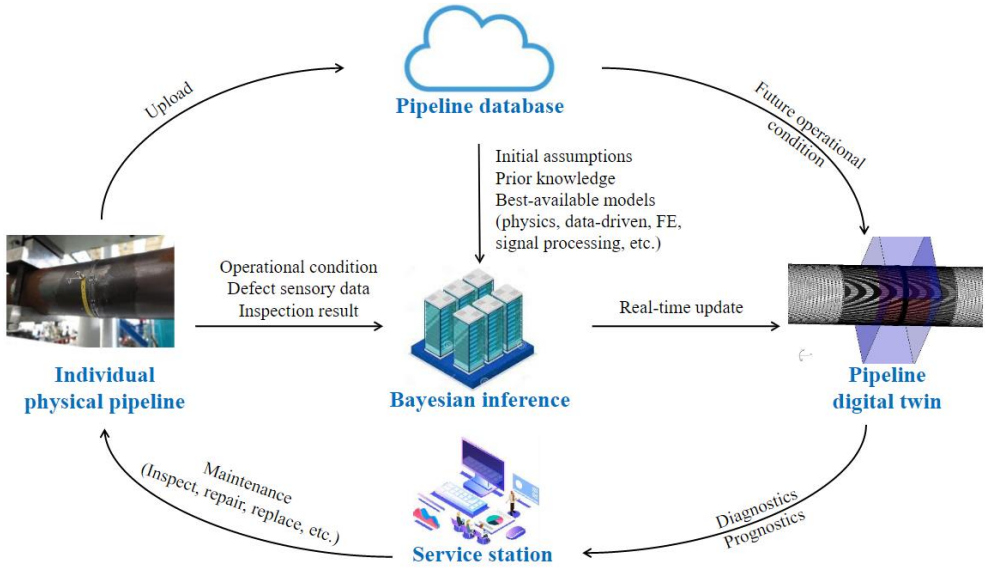

Figure 20: Digital twin ecosystem for pipeline condition monitoring.

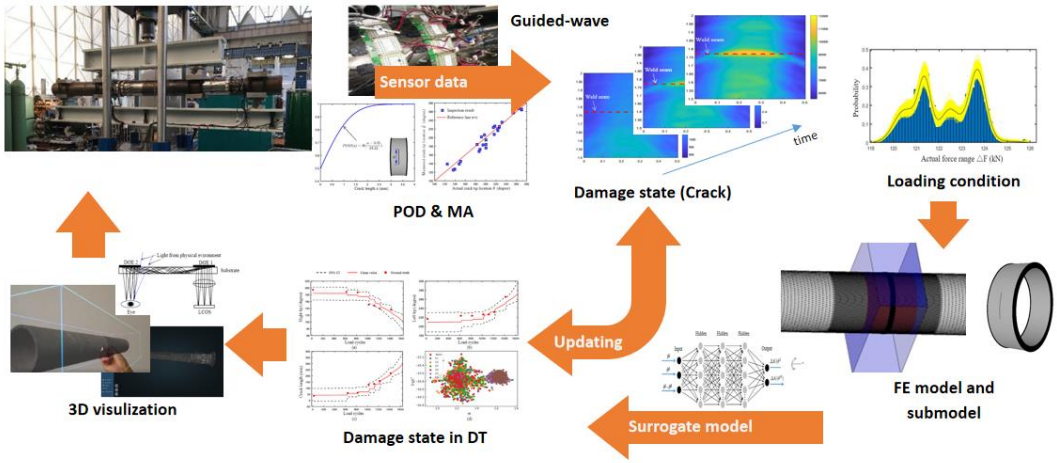

Figure 21: A real-world prototype of the digital twin ecosystem for pipeline condition monitoring

4.4.1 REFERENCES

[10] T. Wang, Z. Liu, M. Liao, and N. Mrad, "Life prediction for aircraft structure based on Bayesian inference: towards a digital twin ecosystem." Annual Conference of the PHM Society. vol. 12, no. 1, pp. 1-8, 11/09/2020-11/13/2020, Virtual conference.

[11] R. N. L. S. T. Gaul, B. Weihnacht, "Localization and quantification of cracks in fatigue tests with guided waves (in German)," DGZFP Annual Conference, vol. 09, pp. 1–8, 22/05/2017-24/05/2017, Koblenz, Germany.

5.0 LOAD, USAGE, AND STRUCTURAL HEALTH MONITORING

5.1 Helicopter Load and Usage Monitoring Research in 2021-2023

Catherine Cheung, NRC Aerospace

5.1.1 ENSEMBLE APPROACHES FOR LEVERAGING MACHINE LEARNING MODELS IN LOAD ESTIMATION

Helicopter component load estimation can be achieved through a variety of machine learning techniques and algorithms. To increase confidence in the load estimation process, ensemble methods, methods that leverage the results of multiple machine learning models to make more informed predictions, are employed. These techniques are beneficial in many domains, namely that they increase predictive stability across subsets of data and add robustness to noisy data. In this work, ensemble integration techniques are investigated for the estimation of main rotor yoke loads using flight state and control system parameters. A range of ensemble integration techniques were implemented, including simple averaging, weighted averaging, and forward selection. Several metrics were trialled to optimize the selection of the top 25 models from a total of 426. When evaluated using the following metrics: the root mean squared error (RMSE), the correlation coefficient, and the interquartile ranges of these two metrics, all of the ensembles of models outperformed the best individual model. Of the techniques explored in this paper, the ensembles using the forward selection technique achieved the best performance with relation to those metrics and its predicted signal visually matched the original signal most closely. The resulting output is more robust, more highly correlated, and achieves similar or lower error values as compared to the top individual models. While individual model outputs can vary significantly, confidence in their results can be greatly increased through the use of a diverse set of models and ensemble techniques. Ensembles compensate for the error distribution of the individual models and reduce the variance of the estimates.

In this work, a large pool of helicopter load estimation models was generated to estimate main rotor yoke loads from 28 flight state and control system parameters. It is important to note that these existing sensors were not originally installed for the purpose of estimating component loads, and attempts to obtain accurate predictions from these sensors require extracting as much relevant information as possible using machine learning models. Five machine learning model types were included, in particular random forest, multi-variate adaptive regression splines, multi-perceptron neural networks, 1-dimensional convolutional neural networks, and long-short term memory recurrent networks. Three load estimation methods were explored, namely the National Research Council of Canada (NRC) baseline prediction method, signal approximation method, and extended signal approximation method. A wide variety of hyperparameter configurations and random seed values were investigated. Individual models were evaluated based on root mean squared error and

correlation with the target signal, as well as, the interquartile ranges of these metrics. Considerable variation in the model results was evident when changing the random seed and hyperparameter configuration. Subset selection based on rank sum and rank product were trialled and then simple average or weighted average ensembles were constructed from the reduced set of models. There were some notable benefits to using a simple ensemble of individual models, in particular introducing diversity in the individual models making up the ensemble in terms of configuration and algorithm, and a smoother load signal prediction with higher correlation. While individual model outputs can vary significantly, the effects can be mitigated using a thoughtful approach to evaluating models and creating subsets and ensembles of models.

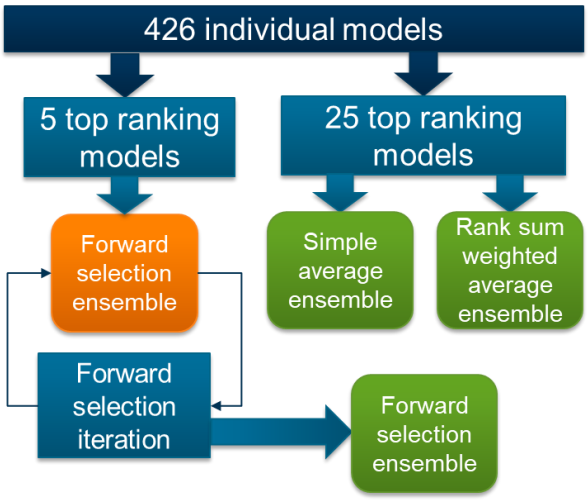

Figure 22: Ensemble construction

From the 426 individual models that were trained, 25 top models were selected based on the ranking metrics. A simple average ensemble, a weighted average ensemble based on rank sum, and a forward selection ensemble were generated, as shown in Figure 22. All ensembles achieved improved performance for these four metrics compared to the best individual models, with the forward selection ensemble obtaining the lowest RMSE, highest correlation, and closest load signal prediction visually of all models. While the simple average and weighted average ensembles relied predominantly on NN-MLP models using BPM, there was much more diversity in the forward selection models, including three model types and both BPM and extSAM load prediction methods. The forward selection approach of considering models based on overall ensemble performance was notable for its improved performance over other ensemble integration methods. The role of metrics in the optimization process in training individual models and building ensembles was another important takeaway from this work.

Developing an approach for managing, selecting and leveraging a large number of machine learning models as well as other solutions is valuable, particularly in the rapidly advancing field of machine learning (ML) and artificial intelligence (AI). Future work will look at including other

machine learning algorithms that provide improved load estimates, particularly at the peaks. Consideration and inclusion of other metrics is also planned to increase the explainability of the machine learning models and to improve the load estimates.

5.1.1.1 REFERENCES

[12] Cheung, C., Biondic, C., Hamaimou, Z., Valdés, J.J., "An approach to merging machine learning models in an ensemble for load estimation", *Proceedings of the 12th DST International Conference on Health and Usage Monitoring*, Melbourne, Australia (virtual), Nov 29-Dec 2, 2021.

[13] C. Cheung and Z. A. Hamaimou, "Ensemble integration methods for load estimation," in *Proceedings of the Vertical Flight Society 78th Annual Forum*, Ft. Worth, Texas, USA, May 2022.

5.1.2 REGIME RECOGNITION – EVALUATION TOOLS AND GROUND TRUTH LABELLING

Regime recognition is an important tool for monitoring aircraft usage. Algorithms for this task are normally trained and tested on flight load survey data. In many instances, significant portions of the flight data are not used because of labelling uncertainties. Flight test data is expensive to generate, but machine learning-based solutions rely on copious amounts of training data, so the idea of discarding data is unappealing. This paper presents a process to consistently and systematically label flight data with common helicopter regimes that would reduce the amount of unlabelled flight test data. The approach makes use of regime descriptions and parameter time histories to assign labels, which are then verified using flight path and flight test card information. Although the implementation of the approach is challenging, the initial results from Bell 206 test flights demonstrate that this approach can significantly reduce the amount of unlabelled flight data, enabling much more usable data for training algorithms.

This work outlines a process for consistently and systematically assigning ground truth labels to flight data. This approach is based on information obtained from the following sources of information:

- Manoeuvre / regime descriptions
- Flight test card / flight log
- Parameter time histories
- Flight path

Basic manoeuvres were considered for this initial work: straight-and-level flight, turns, climb, descent, hovering, takeoff and landing. From the regime description, the key parameters for identifying these manoeuvres were determined: altitude, heading, airspeed, pitch, roll, climb rate, lateral cyclic, longitudinal cyclic, collective, and pedal position. Key attributes or criteria for these parameters, such as whether the values were constant, increasing, decreasing, or had a value of zero were determined to differentiate the regimes. An algorithm was developed to implement these criteria for a total of 33 regimes, which required adjustment to suit the nature of the measurements and parameter data. Labels to the flight data were then assigned based on these criteria. The

parameter time histories, the flight path and flight test card were used to verify and validate the assigned labels.

This approach was applied to flight test data obtained from two short Bell 206 flights. Due to the lack of control input data in the Bell 206's inertial navigation system and some issues encountered with the sensor measurements (heading, airspeed), the parameters used for labelling the regimes were restricted to altitude, pitch angle, roll angle, climb rate, and roll rate. Despite these limitations, the algorithm implementing the criteria for regime labels led to a significant increase in the amount of labelled data for these flights. Comparison with previous results (Figure 23) shows that using this approach to label the data, the amount of unlabelled data could be reduced to less than 10% (from 49.6% and 92% unlabelled) as shown in Figure 24, which is a dramatic improvement. Further analysis and adjustment to the algorithm for assigning labels to these flights is still necessary, but the initial results are extremely promising. The fact that the algorithm provides a clear record of how the labels were assigned is valuable in itself, so that further analysis and explanation of certain labels can be easily obtained.

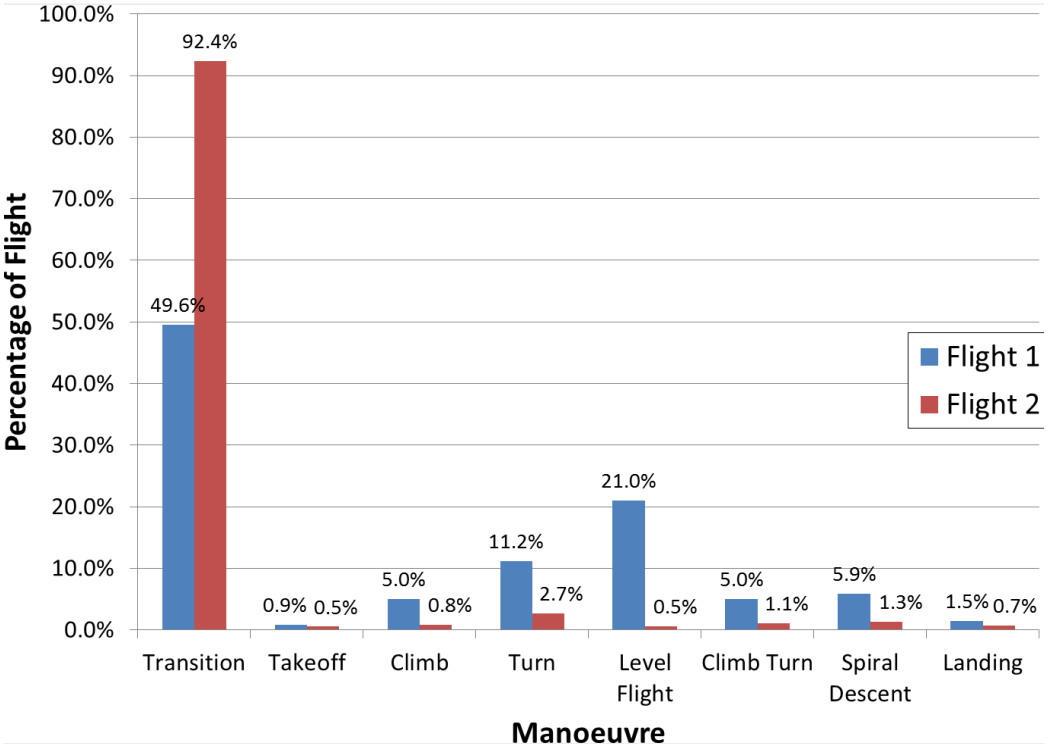

Figure 23: Original distribution of flight data by manoeuvre

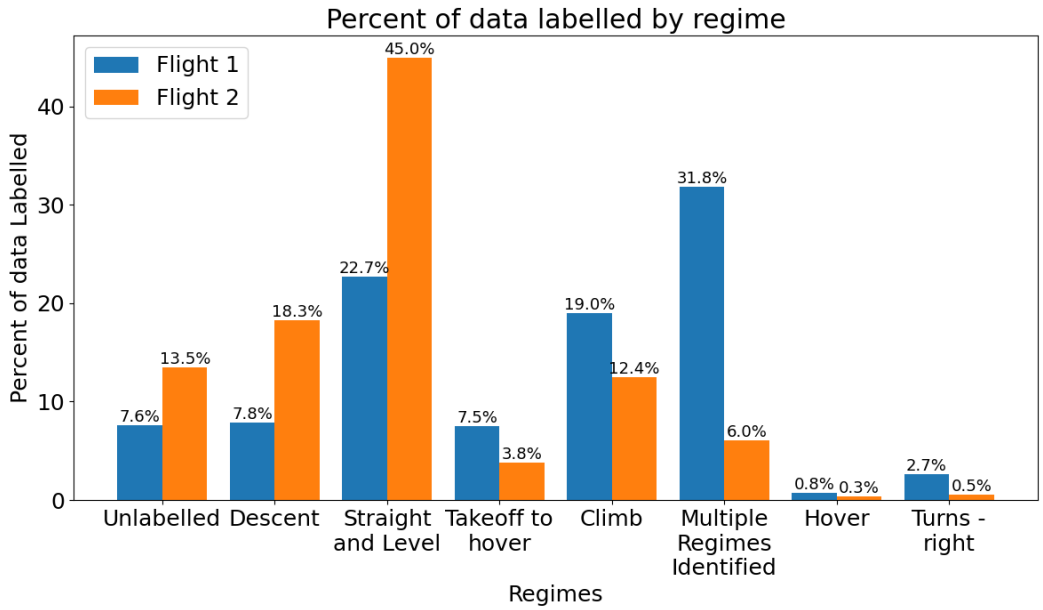

Figure 24: Revised distribution of flight data by manoeuvre after labelling approach

5.1.2.1 REFERENCES

[14] C. Cheung, E. Seabrook, "Towards an Evaluation Process for Regime Recognition Approaches: Addressing Variability in Labeling Training Data" in *Proceedings of the Vertical Flight Society 79th Annual Forum*, West Palm Beach, FL, USA, May 2023.

5.1.3 SAE HM-1R HUMS DATA STANDARD

The SAE HM-1R Rotorcraft Integrated Vehicle Health Management committee was formed with the intent of establishing a consensus standard data format for health and usage data within the commercial and military rotorcraft community. Current health and usage monitoring systems (HUMS) used in commercial and military rotorcraft use proprietary data formats for downloaded data. Such approaches limit the ability of operators to analyze the data outside of the tools and information provided by the HUMS supplier. The goal of the standard is to provide a data format applicable to the needs of future rotorcraft, such as the US Army Future Vertical Lift (FVL) program. As well, it is intended to provide a data format that can accommodate translation of existing HUMS data into the new format to encourage broader adoption, Figure 25. Committee participants include representatives from major helicopter original equipment manufacturers (OEMs) (Bell, Sikorsky, Boeing, Leonardo), primary HUMS suppliers (GE, Collins, Honeywell, Rolls Royce), certification agencies (FAA, EASA), US military programs (US Army, US Air Force), research organizations (NRC, DSTG), and others.

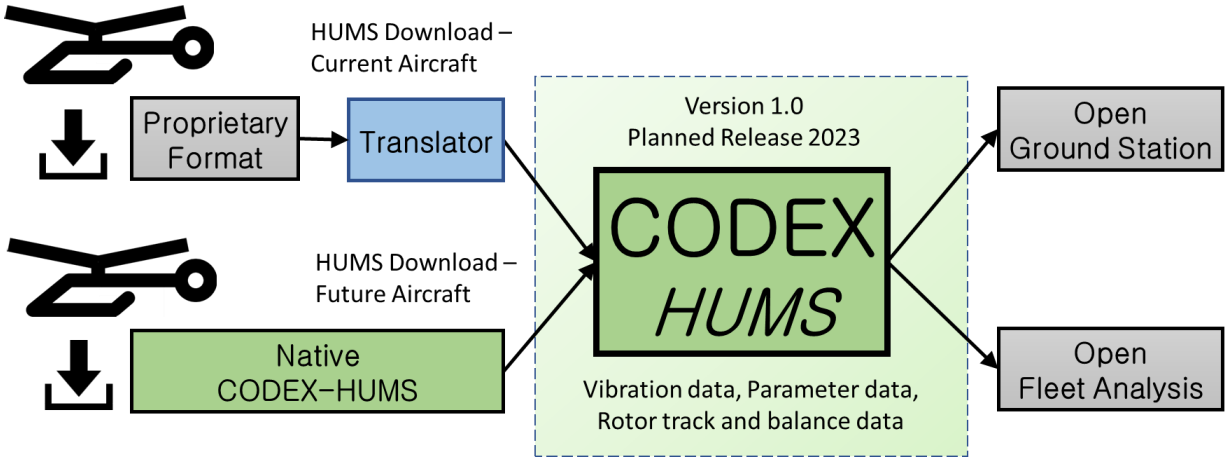

Figure 25: Applying CODEX-HUMS format to both current and future aircraft (SAE HM-1R Subcommittee)

5.1.3.1 REFERENCES

[15] T. Royar, B. Tucker, C. Cheung, "Opening the Book on HUMS Data", *Vertiflite*, Vol. 69, No. 3, Vertical Flight Society, Fairfax, VA, May 2023.

5.2 CT-142 Operational Loads and Engine Monitoring System

Stephane Brunet, NRC Aerospace

The CT-142 aircraft is a military version of the De Havilland Canada DHC-8-100 used by the Royal Canadian Air Force (RCAF) for air navigation training. The current role of this aircraft differs significantly from the original commercial transport role for which the DHC-8-100 was certified. As a result, the Original Equipment Manufacturer (Bombardier, at that time) conducted an assessment of the additional fatigue damage induced on the aircraft structure due to its new role. For this purpose, the vertical acceleration data was recorded during a full calendar year on one instrumented aircraft. Subsequent data analysis enabled the quantification of fatigue damage on the CT-142 in comparison to the commercial version.

Almost two decades later, the mission profiles flown by the CT-142 aircraft have changed and the RCAF would like to re-evaluate the actual usage and its impact on the fatigue damage on the structure. The RCAF therefore mandated NRC to develop an Operational Loads Monitoring System (OLMS) to be installed on one or more of the fleet aircraft, for continuous recording of the vertical acceleration during every flight. Data processing, which would follow a similar process used until recently on the CC-115 Buffalo, would be done on a regular basis and permit an accurate evaluation of the accrued fatigue damage induced on the aircraft.

The OLMS hardware is built around an Inertia Measurement Unit (IMU), which captures linear accelerations, rate of rotations and Earth's magnetic field vector components in all three axes. The IMU output data is captured by a National Instruments standalone controller, which applies a timestamp and records the data on flash memory for later download and offline processing. A single prototype OLMS is to be installed on one aircraft for initial testing in Fall 2023. Following this, the option to instrument the remaining fleet will then be evaluated.

In parallel to the structural OLMS, the RCAF also tasked NRC to evaluate the feasibility of integrating the data collection of engine parameters required for health monitoring of the two PW120 turboprop engines. Currently, the crew collects a set of parameters manually on a paper form at one single and specific time during the flight. As this method has several drawbacks, an autonomous data collection system which would continuously record engine parameters during all flights would be desirable. Considering the customization possibilities offered by the standalone controller used for the OLMS, NRC has shown that the engine data collection feature could be added to the current OLMS system. The results of this engine monitoring feasibility study are currently under review at the RCAF.

Figure 26: CT-142 (Dash-8, https://www.canada.ca/en/air-force/services/aircraft/ct-142.html)

6.0 NON-DESTRUCTIVE EVALUATION

6.1 Robotized Ultrasonic Phased Array C-Scan

L3Harris - Military Aircraft Services (MAS)

Over the last decades, L3 Harris MAS has launched several research and development initiatives to support the various In-Service Support (ISS) contracts that it supports. Many of these efforts pertain to software development for fatigue damage evaluation and the management of life limiting items. The other area where MAS has succeeded to bring innovative technologies to market is robotics, more specifically shot peening and machining. The Robotized Ultrasonic Phased Array C-Scan capability is the latest of those technologies.

The system is designed to produce Ultrasonic C-Scans for air-control surfaces for the CF-188 and CT-114 aircraft. Two collaborative robots are mounted on a gantry–type structure (Figure 27) that can be moved to the aircraft location. Custom phase-array probes (Figure 28) containing up to 64 elements sweep across the surfaces collecting ultrasonic data through three separate channels. Two Pulse-Echo channels analyse the top and bottom skins for disbonds and delamination, and a Through-Transmission channel verifies the bonding of the sandwich assembly.

The process, based on a CT-114 elevator bonded assembly, is being finalized and will be submitted to the Department of National Defence of Canada for certification.

Figure 27: Robotized ultrasonic phased array C-Scan arrangement

The data is post-processed to identify the type of flaw and compare the scan to previous scans or the scan of a nominal part. The ultrasonic data is stored for future investigation. The system solves multiple technical difficulties such as robot synchronization, probe alignment, surface roughness, ultrasonic coupling, contact pressure, etc.

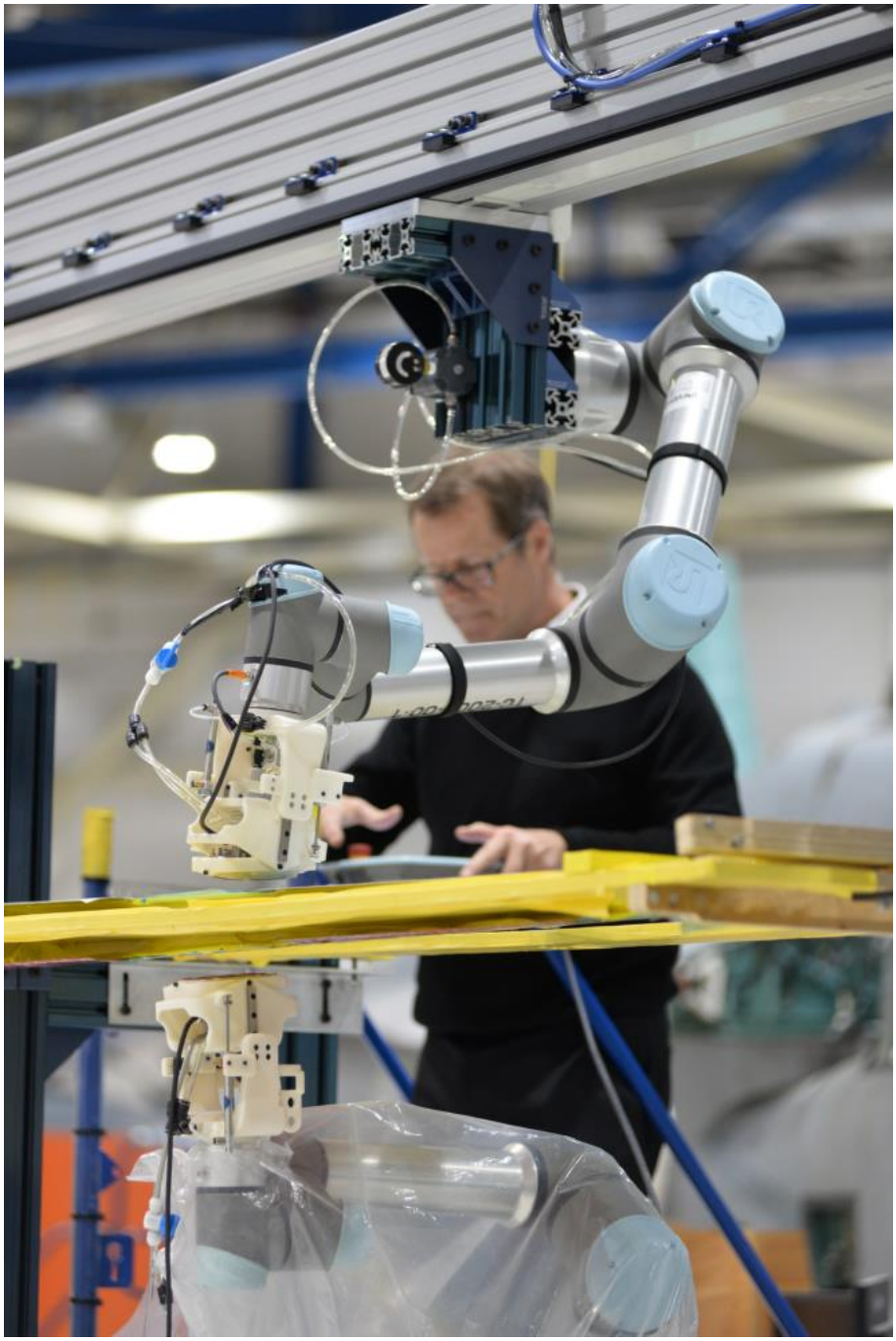

Figure 28: Robotized ultrasonic phased array C-Scan sensors

A custom user interface manages the sequence of operations and prompts the operator for manual operations (Figure 29).

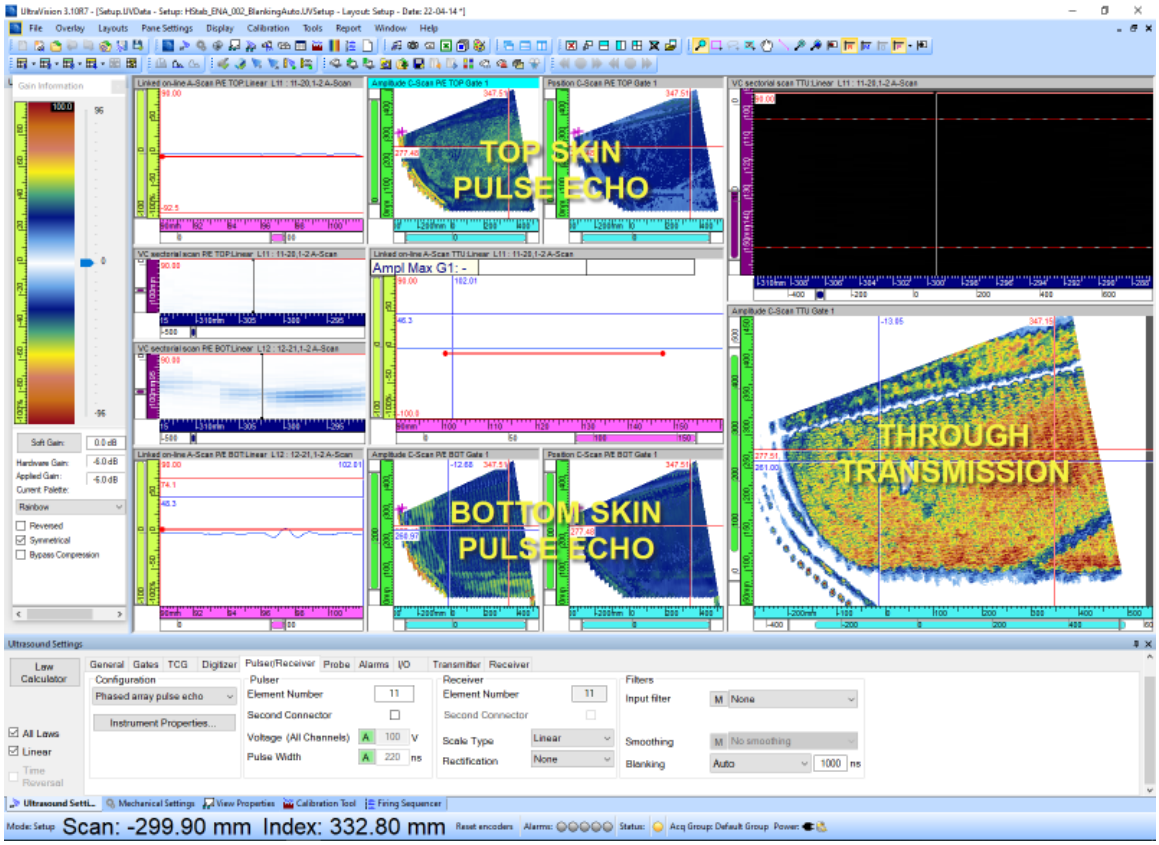

Figure 29: Robotized ultrasonic phased array C-Scan imaging

6.2 In-Situ Crack Growth Monitoring with Structure-Bonded Eddy Current Coils

Catalin Mandache, NRC Aerospace

Structural health monitoring (SHM) applied for strain, vibration, and temperature measurements (strain gauges, accelerometers, thermocouples) are not meant to detect damage. On the other hand, SHM sensors for damage detection have the role of in-situ non-destructive inspections (as for diagnosis) and on-line monitoring for preventive measures (as for prognosis). Condition-based monitoring is a required component of predictive maintenance and has the potential of increasing availability and maintaining safety of metallic structures while reducing costs associated with

periodic inspections. Also, it has to be considered for parts and components not designed for inspectability.

In-situ non-destructive evaluation uses sensors that could accurately monitor the condition of aircraft structures without causing disruptions to service, necessitating disassembly, or introducing inadvertent damage.

The use of embedded eddy current sensors for condition assessment and monitoring is still in its incipient stages. However, it has been demonstrated that thin and flexible eddy current coils of less than 100 μm in thickness (Figure 30) are useable for in-situ detection and monitoring of fatigue cracks in metallic aircraft structures, with promising prospective for crack sizing [16]. The coils are minimally invasive and could be attached to or embedded into the evaluated structure. When placed in critical areas, such around the fastener holes, they could monitor the growth of radial fatigue cracks, as demonstrated in the results shown in Figure 31 [16] [17]. The relative impedance change of the crack monitoring coil with respect to an identical coil placed on a reference specimen/location was chosen as the appropriate feature of interest, based on practical applicability, as well as, sensitivity to crack growth. In the same time, a flexible bonding material was chosen to increase the coil survivability in the strain field of the crack.

Figure 30: Instrumented fatigue test coupon

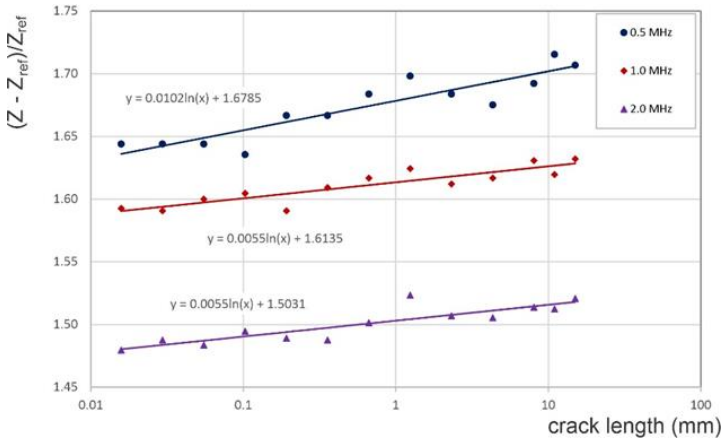

Figure 31: Crack growth monitoring based on the relative change in the Coil's impedance. Lower frequencies displayed better sensitivities

6.2.1 REFERENCES

[16] Catalin Mandache, Richard Desnoyers, Yan Bombardier, "Crack growth monitoring with structure-bonded thin and flexible coils", Sensors 2022, Volume 22, Issue 24, 9958.

[17] Catalin Mandache, "Structure-bonded flexible eddy current coils for in-situ crack monitoring", 10th European Workshop on Structural Health Monitoring, Palermo, Italy, July 3-7, 2022.

6.3 Inspection of a Helicopter Blade using Drone Based Active Thermography

Shashank Pant[1], Marc Genest[1], Clemente Ibarra-Castanedo[2], Nicolas P. Avdelidis[2,4], Julio Valdes[3], Shakeb Deane[4], Argyrios Zolotas[4], and Xavier P. Maldague[2]
[1] NRC Aerospace
[2]Computer Vision and Systems Laboratory, Department of Electrical and Computer Engineering, Laval University, Quebec City, Quebec, G1V 0A6, Canada
[3] NRC Digital Technology Research Center
[4]School of Aerospace, Transport and Manufacturing, Cranfield University, Cranfield, MK43 0AL, UK

A drone-based inspection system that can move "freely" around an aircraft to perform the inspection of all the areas of interest in a fast and effective manner can have significant impact in reducing inspection time and cost. In this work, a commercially available DJI Mavic 2 Enterprise Advanced drone equipped with both thermal and optical cameras was used to inspect an out of service Main Rotor Blade (MRB) of a Bell 412 helicopter, as shown in Figure 32. The drone was navigated manually by a pilot in an indoor facility by maintaining a height of approximately 0.5 meter above the specimen, while acquiring the thermal and optical footage. Since the drone IR camera when used in the video mode is not radiometric and only provides RGB value from an

MP4 video, a grayscale colormap was selected in the drone IR camera setting for ease of post-processing.

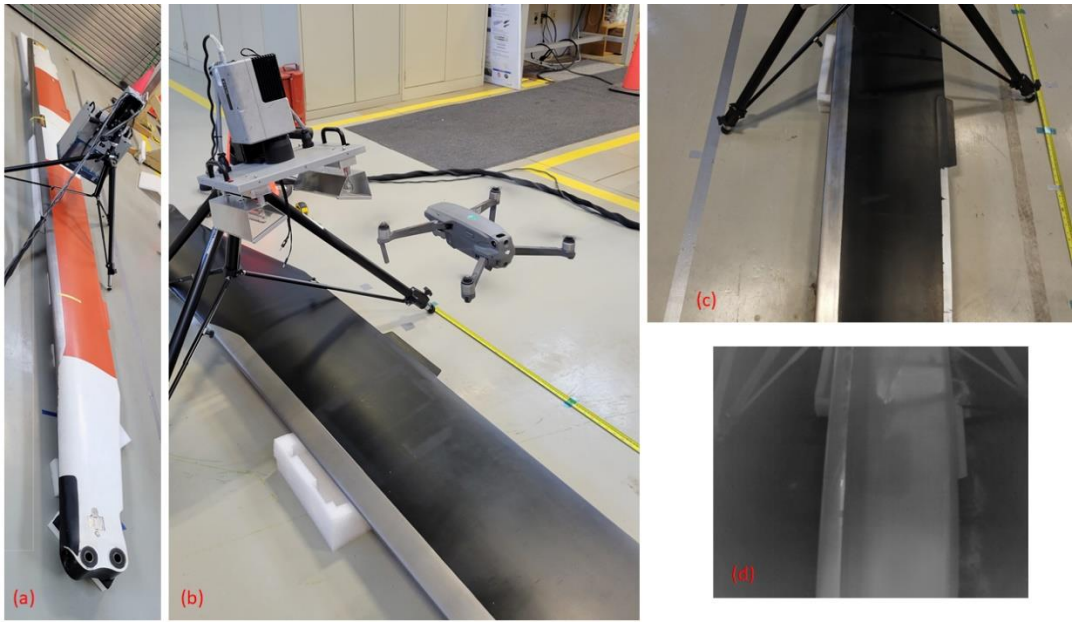

Figure 32: (a) Entire blade, (b) experimental setup, (c) optical image, and (d) thermal image acquired from the drone's camera

Drones are inherently unstable, thus any videos acquired from a drone's camera will have some degrees of undesired motion even with on-board stabilization and gimbals. For stabilizing the videos acquired from the drone, a procedure previously developed by the authors was used with an addition of z direction (zoom) for complete stabilization. The un-stabilized and stabilized thermal sequences were processed using typical signal processing techniques used in pulsed thermography such as pulsed phase thermography (PPT) and principal component analysis (PCA) thermography, results of which are shown in Figure 33 and Figure 34.

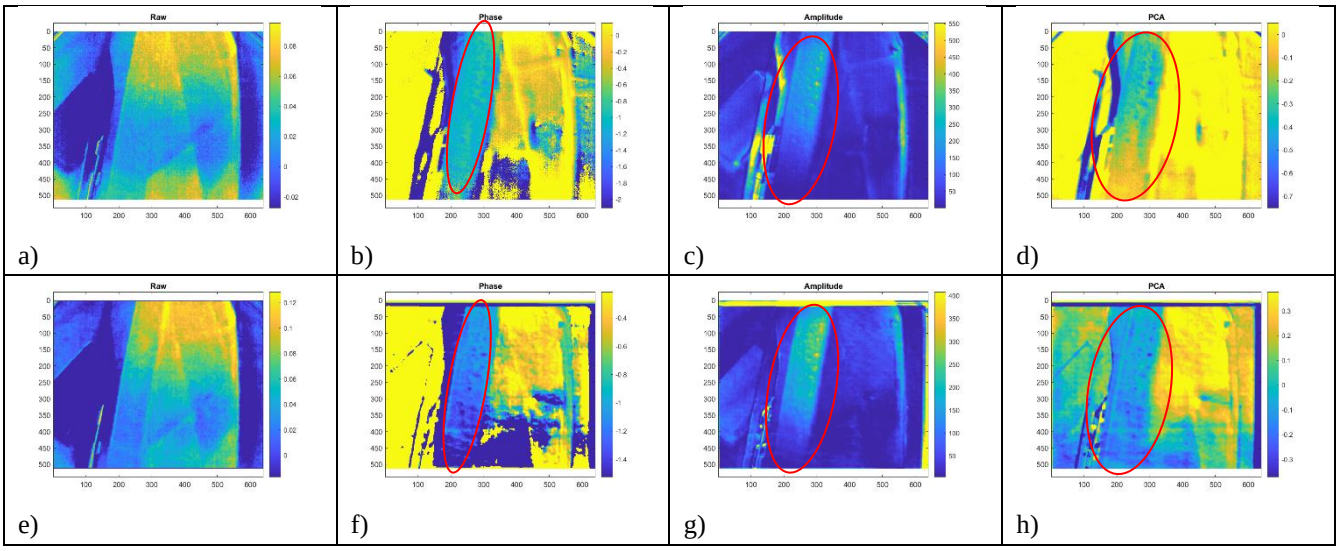

Figure 33: Unstabilized top-row: a) raw image of a single frame, b) phase image, c) amplitude image, d) PCA first component; stabilized bottom-row: e) raw image of a single frame, f) phase image, g) amplitude image, h) PCA first component

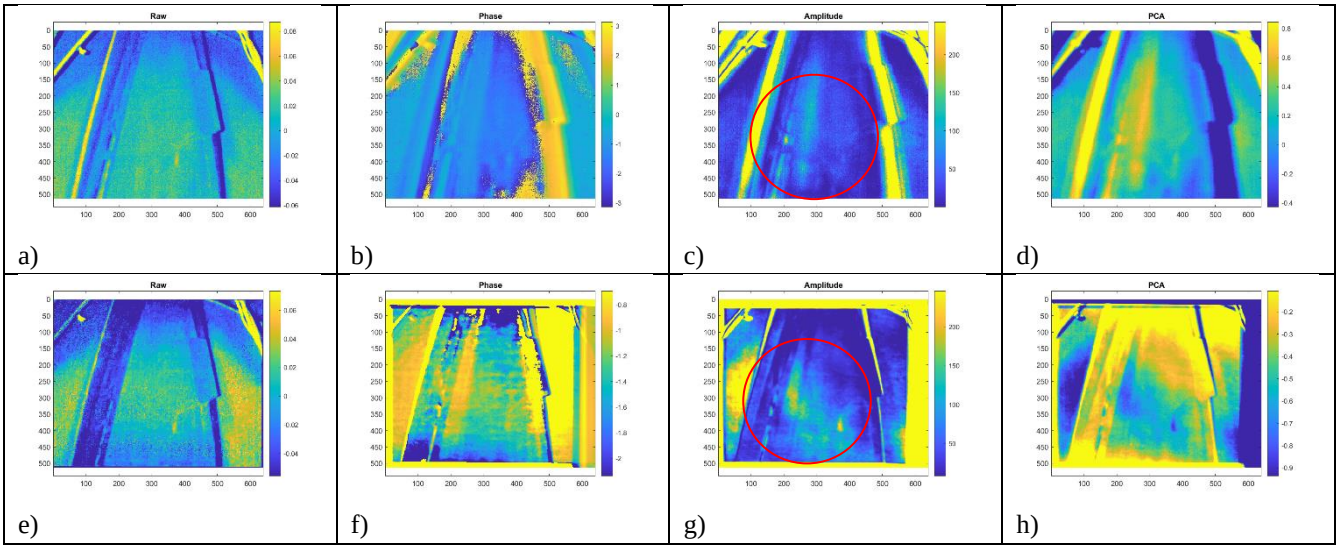

Figure 34: Unstabilized top-row: a) raw image of a single frame, b) phase image, c) amplitude image, d) PCA first component; stabilized bottom-row: e) raw image of a single frame, f) phase image, g) amplitude image, h) PCA first component

In the figures above, it can be seen that raw unprocessed thermal data can be used to see shallow and large thermal anomalies from the structure. For deeper anomalies and features with faint thermal signatures, the stabilized version resulted in much sharper edge definition and better overall detection as compared to the un-stabilized version. In Figure 33, more voids or access

adhesive pockets, at the leading edge of the MRB (area circled in red), are discernible in the stabilized version. Whereas, in Figure 34, deeper anomalies were better seen in the stabilized sequence as highlighted by the red circle. Therefore, this work demonstrated the possibility of drone based active thermography inspection. However, further development such as: incorporating powerful heating source on-board the drone to provide ample thermal gradient without affecting or blocking the field of view and autonomous capabilities are required for full utilization of this novel technique.

6.3.1 REFERENCES

[18] S. Pant, M. Genest, C. Ibarra-Castanedo, N. P. Avdelidis, J. Valdes, S. Deane, A. Zolotas, and X. P. Maldague, Inspection of a helicopter blade using drone based active thermography, SPIE Defense+ Commercial sensing, Thermosense: Thermal Infrared Applications, Mar 2023.

6.4 Human Factor Effects on Nondestructive Inspection of Aerospace Structures

Muzibur Khan, NRC Aerospace

Early crack detection in aircraft structural components is of extreme importance because cracks that begin at the microscopic scale can propagate under fatigue loading, reach a critical state and eventually cause a structural failure. In aeronautical structures maintenance, nondestructive inspections are commonly used to detect cracks before they reach the critical size. Reliable detection capability of a nondestructive evaluation (NDE) procedure is commonly measured by the Probability of Detection (POD), which is generally expressed as a curve with a specified confidence level of detecting a flaw against its characteristic parameter (usually its size). The POD data is extremely important, especially in Damage Tolerance Analysis (DTA) and when newly developed inspection procedures are deployed into fleets. The POD is considered as a quantitative measure of the reliability of a chosen NDE procedure. Conventional POD analysis methodologies, as described in MIL-HDBK-1823A, require designing and manufacturing a statistically valid number of specimens from a representative material, with an induced discontinuity and taking into account equipment variability. Experiments are designed in order to generate a required distribution of crack inspection data (hit or miss) for statistical analysis to estimate the probability of detection. The reliable detectable crack (defect) size and probability of detection depend on a number of variables that influence the NDE outcome, such as crack size, location, orientation, inspection system/equipment, geometry, material, and data acquisition processes. The inspection environment, the ability, and attitude of the NDE inspector, commonly termed as human factors, also have a great influence on reliability. It has been demonstrated from cross-industry trials and experience that the reliability of NDE inspection can be significantly affected by human

performance issues. However, human factors do not receive much attention in NDE reliability assessment.

In the past, the National Research Council of Canada (NRC) carried out a project aimed at generating data and estimate the POD of fatigue cracks in bolt holes of aircraft wing structures. The sites targeted for this POD study were fastener bolt holes of wing skin splices, spar-to-web and skin-to-spar joints of the military aircraft (CC-130 and CP-140). A generic rotating bolt hole eddy current inspection procedure was employed for detecting fatigue cracks, as well as, electric discharge machined (EDM) notches in target sites. The wing components were simulated by manufacturing simple two-layer test coupons, referred to as inspection sets, with a centrally located bolt hole (Figure 36). In this POD study, the inspection was performed for four different inspection configurations based on location of cracks and EDM notches in a two-layer setup. The inspection was performed using a test procedure developed for this study based on eddy current inspection (single point calibration) practices for bolt hole inspection, and inspection results were recorded in terms of "hit-miss" data (crack found Yes/No), as well as, the eddy current signal amplitudes or "a-hat" (as number of graticules or % of screen height). The discontinuity types (fatigue cracks and EDM notches) and statistical models performed were reported [19].

Ideally, for a particular NDE application setup, all cracks of the same length should have the same detection probability. From this study, the variation in inspection results among different inspectors has been observed although the inspections were performed in laboratory conditions according to common well-defined standard instructions, parameters and qualified personnel (experience from one year to twenty-three years). This study also demonstrated considerable differences between qualified inspectors in their abilities to find defects that could not be explained by the inspector skill level, education, training (initial or recurring), or age (Figure 36 and Figure 37). The extent of variation was as large as 300% in some cases. Recently, the human factor effects on bolt hole eddy current inspection were analyzed and reported [20]. The prime influence of such large variation was largely attributed to the human factors and caused by differences in calibration (ex. gain setting, phase angle, nulling error in eddy current instrument), alignment of the probe in the most responsive location, lift-off variations caused by the probe tilt or wobbling, probe manipulation, signal interpretation by the individual inspectors etc. (Figure 38).

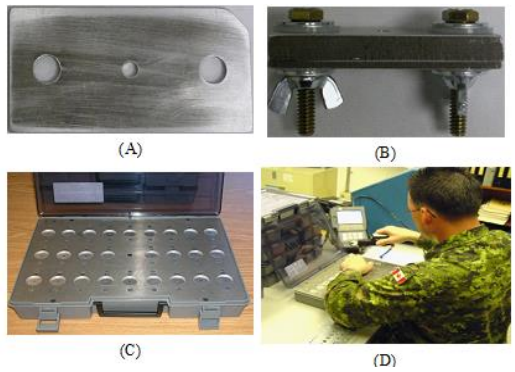

Figure 35: Single test coupons (A), Inspection set side view (B) Inspection set assembled in box (C), inspector performing eddy current inspection (D)

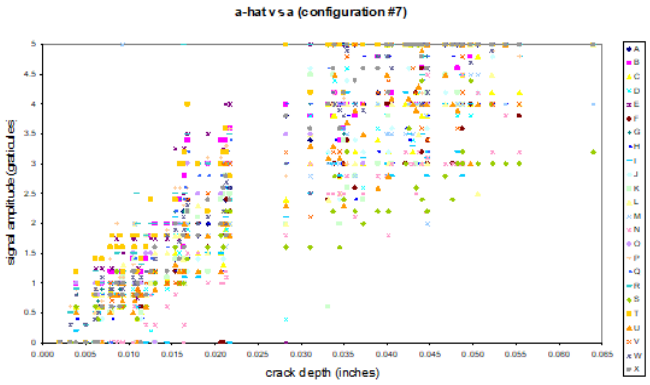

Figure 36: Variation of signal amplitude measured by different inspectors

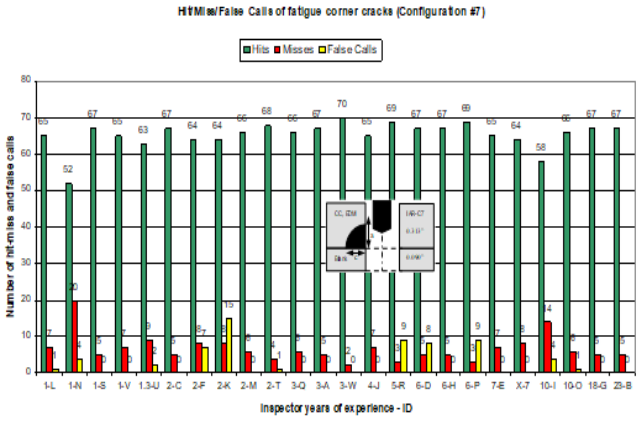

Figure 37: Histogram of Hit/Miss/False Calls of corner cracks (24 inspector, 1 to 23 years of experience)

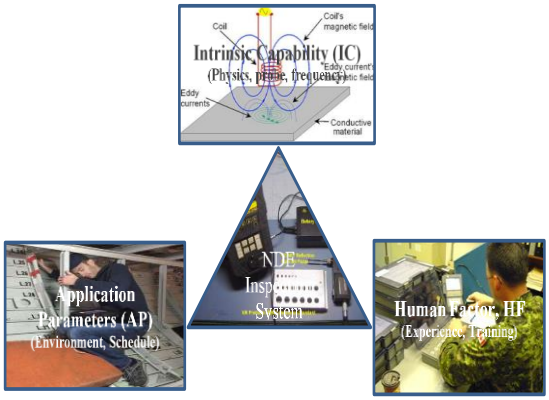

Figure 38: Modular model of NDE reliability for bolt hole inspection

6.4.1 REFERENCES

[19] Khan, M., Yanishevsky, M., and Fahr, A., "Bolt Hole Eddy Current Testing Probability of Detection, Part - I: Experimental Design and Data Analysis, Proceedings of 12th International Conference on Fracture, Ottawa, July, 12-17, 2009.

[20] Khan, M., Genest, M., "Human Factor Effects on Nondestructive Inspection of Aerospace Structures", Proceeding of the 16th Asia Pacific Conference for Non-Destructive Testing (APCNDT), Melbourne, Australia, February 2023.

7.0 FATIGUE AND STRUCTURAL INTEGRITY OF COMPOSITES

7.1 High-Fidelity Simulation of Low-Velocity Impact Damage in Fibre-Reinforced Composites *

Lucy Li[1], Peyman Shabani[2], Jeremy Laliberte[2], Gang Qi[1]
[1] NRC Aerospace
[2] Department of Mechanical and Aerospace Engineering, Carleton University, Canada
* Full paper being presented at ICAF2023

The next revolution in aviation is driven by virtual testing and digital twinning for aircraft design, development, certification, and sustainment. The cornerstone of the digital evolution to accelerate aircraft development and certification, and to adapt predictive maintenance and lifing, is reliable and accurate numerical models to provide insight into usage, performance, residual life, and other states of the aircraft. High-fidelity finite element models are proven to provide an accurate and physics-based prediction of composite progressive damage, which support design optimization or maintenance actions.

In this study, a high-fidelity three-dimensional (3-D) finite element (FE) model was developed to accurately predict ply-by-ply damage sizes and failure modes interactions in composite laminates during a low-velocity impact (LVI) event. To predict different failure modes, the cohesive zone modelling (CZM) technique and the LaRC05 failure criteria were employed. Cohesive layers were deployed between each adjacent composite ply to predict delamination. In addition, cohesive elements were embedded inside the composite plies to predict the delamination and matrix cracking interactions and delamination migration from one layer to another. The LaRC05 failure criteria, along with an efficient search algorithm for finding matrix fracture plane and fibre kink-band angle, were employed using a VUMAT user-defined material subroutine in Abaqus to account for matrix cracking, fibre breakage, fibre splitting, and fibre kinking. The flowchart of the VUMAT is shown in Figure 39.

The assembly of the FE model is shown in Figure 40a and Figure 40b. A 254 mm by 304.8 mm (10 in by 12 in) carbon/epoxy (IM7/977-3) composite laminate with a stacking sequence of $[0/45/90/-45]_{4s}$ was modelled in Abaqus. This laminate was impacted by a hemispherical impactor with a diameter of 15.87 mm moving with an initial kinetic energy of 30 J. The support plate and impactor were considered rigid bodies. Four rubber cylinders were modelled to simulate the clamps and the rigid body movement of the laminate was constrained in the X and Y (in-plane) directions by defining contacts between the edges of the laminate and three pins of the support plate. To predict delamination and intralaminar matrix cracking, cohesive elements with a bilinear traction-separation constitutive relationship were employed between each adjacent composite ply and also inside each ply, as shown in Figure 40c. The intralaminar cohesive elements were

embedded with a 45° angle to the thickness of the laminate according to the experimental observations [21]. The damage initiation in the cohesive elements was determined by the quadratic stress criterion and the damage evolution was governed by the power law damage evolution criterion [22].

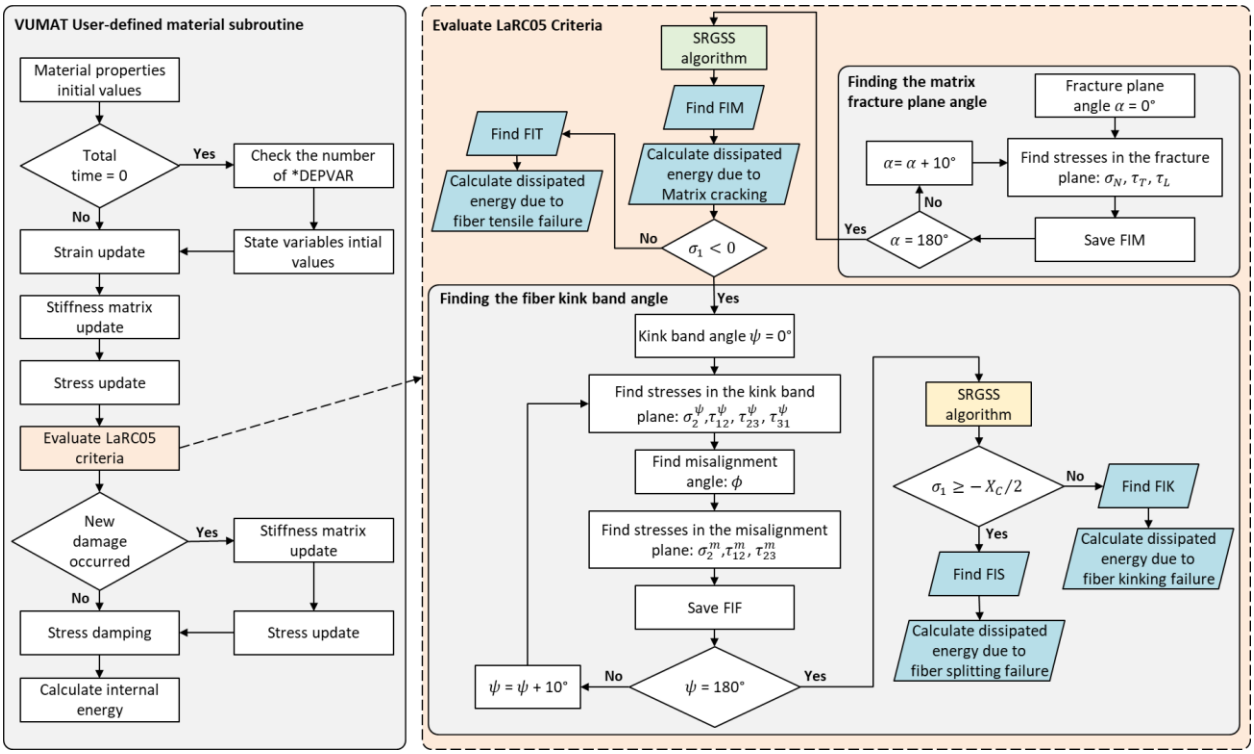

Figure 39: Flowchart of the VUMAT subroutine developed based on LaRC05 failure criteria and SRGSS search algorithm.

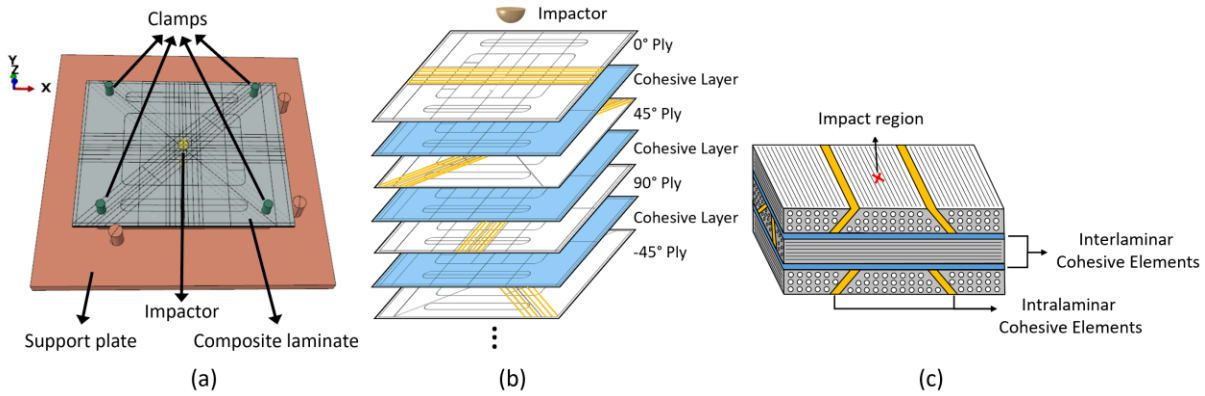

Figure 40: (a) Assembly of the LVI FE model, (b) Layup configuration, (c) Schematic of the cohesive elements employed in the FE model.

The predicted ply-by-ply damaged areas for the $[0/45/90/-45]_{4s}$ laminate after a 30 J impact event are shown in Figure 41. The first row shows the matrix cracking. The matrix cracks after a low-velocity impact event would appear either because of the shear stresses near the impacted surface or because of the high tensile stress perpendicular to the fibre direction near the back face of the laminate [22]. The area of the matrix cracking increased from the impacted surface to the back surface. Although the fibre tensile failure index increased as moving from the neutral plane to the back face of the laminate, it did not reach the value of 1 in any of the elements. Therefore, the occurrence of fibre tensile failure was not predicted for the laminate under 30 J impact. However, fibre splitting and a very small area of fibre kinking were captured near the impacted surface due to high local shear and compressive stresses. The layer-by-layer delamination areas were also predicted as shown in the last row of Figure 41.

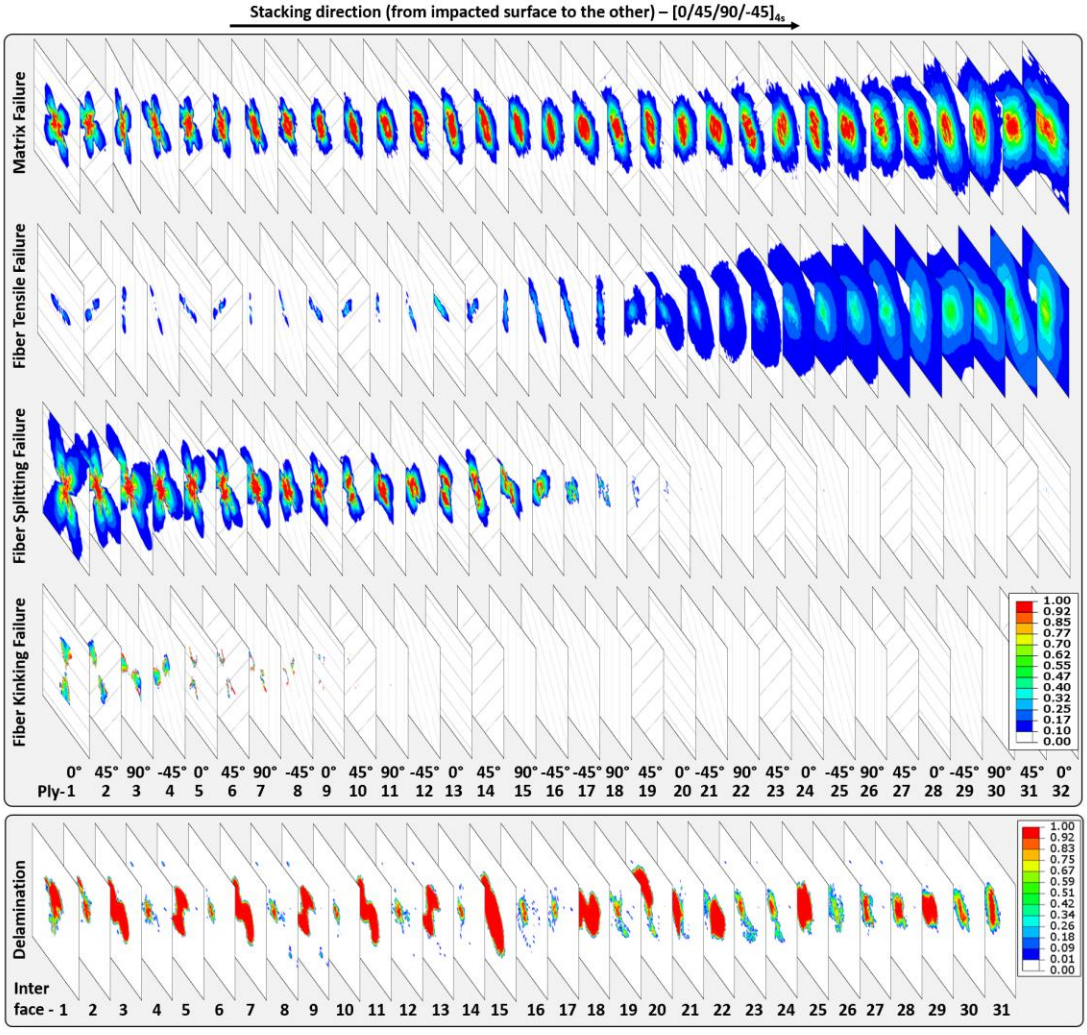

Figure 41: The ply-by-ply predicted damage areas. Each image shows a 40 mm by 40 mm area surrounding the impacted region.

The predicted low-velocity impact response of the laminate and the drop-weigh test results are shown in Figure 42. By comparing the force-time diagram of the experimental results, it was observed that the FE model was not only able to capture the overall response, it also predicted the major peaks and valleys of the load history with good accuracy. A comparison of the key parameters was made between the FE and experimental results as shown in Figure 42. The predicted absorbed energy, total (projected) damage area and peak load were 7%, 10%, and 5% higher than those in the experiment, respectively, and the predicted maximum deflection and contact time were 1% lower than in the experiment.

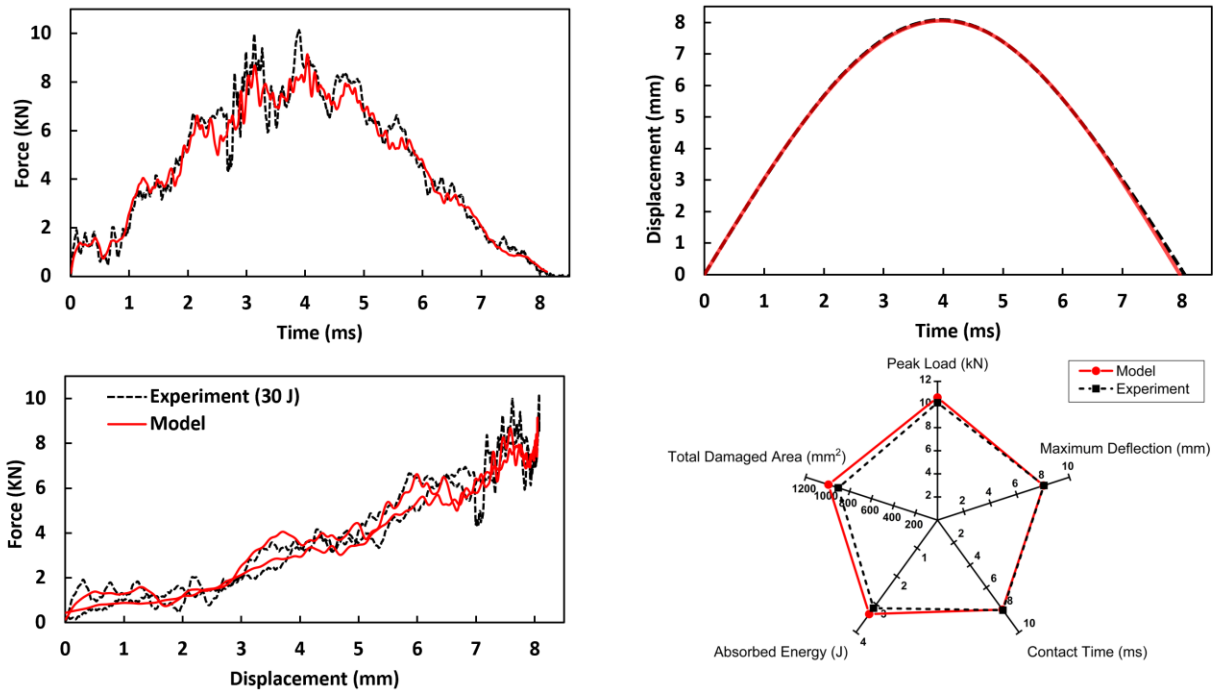

Figure 42: Comparisons of the impact response between the FE model and the experimental results

7.1.1 REFERENCES

[21] M. McElroy, W. Jackson, R. Olsson, P. Hellström, S. Tsampas, and M. Pankow, "Interaction of delaminations and matrix cracks in a CFRP plate, Part I: A test method for model validation," Compos. Part A Appl. Sci. Manuf., vol. 103, pp. 314–326, 2017.

[22] P. Shabani, L. Li, J. Laliberte, G. Qi, D. Rapking, and D. Mollenhauer, "High-fidelity simulation of low-velocity impact damage in fiber-reinforced composite laminates using integrated discrete and continuum damage models," Compos. Struct., p. 116910, 2023.

7.2 AI/ML Enabled Characterization of Thermoplastic Composites

Hamed Esmaeili, Reza Rizvi, Department of Mechanical Engineering, Lassonde School of Engineering, York University, Toronto, ON.

The global thermoplastic composites market was valued at over $17.4 billion in 2022, and is anticipated to expand at a compound annual growth rate (CAGR) of 4.7%, exceeding $23 billion by 2028 [23]. According to a survey by Applied Market Research in 2019, the Aerospace & Defense segment held the largest revenue share in this market [24]. Thermoplastic composites offer several advantages and are primarily used to reduce weight and corrosion in aircraft structures [24]. Experts of Composites Forecasts & Consulting LLC estimate that thermoplastic composites have the potential to reduce aircraft fuel consumption by 10,000 to 72,000 gallons annually, resulting in significant cost savings for fleet operation companies (Table 1) [25].

Table 1: Annual fuel burn savings from each pound of weight reduction [25]

Aircraft Type	Fuel Burn Savings
Regional Turboprops	$185 - 360/year
Regional Jets	$175 – 432/year
Single-Aisle Jets	$150 – 450/year
Twin-Aisle Jets	$175 – 660/year
Jumbo Jets	$440 – 715/year

Despite advantages offered by thermoplastic composites, their utilization poses unavoidable challenges due to a wide range of compositional design possibilities and the complex, non-linear properties of the polymer matrix. This leads to countless structure-property relationships, necessitating extensive physical experimentation. The time-consuming, laborious and costly mechanical characterization tests have hindered the complete realization of the potential of composite materials. Therefore, to alleviate the burden of physical testing, the ability to predict properties of composites based on a limited number of experiments is crucial.

To tackle this issue, one approach is to use physics-based or semi-empirical models which provide knowledge in the form of constitutive laws. However, these models require significant human effort and domain expertise, and in most cases, are complex and impractical. While numerical and physical simulations can support analytical solutions, those methods rely on the representative volume element (RVE) analysis and often fail to generalize similar domain problems.

In the light of recent advancements in machine learning, our team at York University has embraced the opportunity to capitalize on data-driven approaches for characterizing mechanical properties of polymer composites. As a part of a broader effort in collaboration with an industrial partner, we investigated the feasibility of using data-driven models to predict stress-strain curves of

thermoplastic composites with data collected from an open-source database. The models were fine-tuned to accurately predict the complete stress-strain curves of composites based on their composition (filler content), environmental and testing conditions (temperature, etc.). We assessed and optimized the models for prediction accuracy, generalization ability and training time. Our findings revealed that relying solely on an individual complex model does not always yield desired outcomes. Instead, employing an ensemble of simple yet relevant models could not only enhance prediction accuracy and generalization ability but also significantly reduces training time (Figure 43).

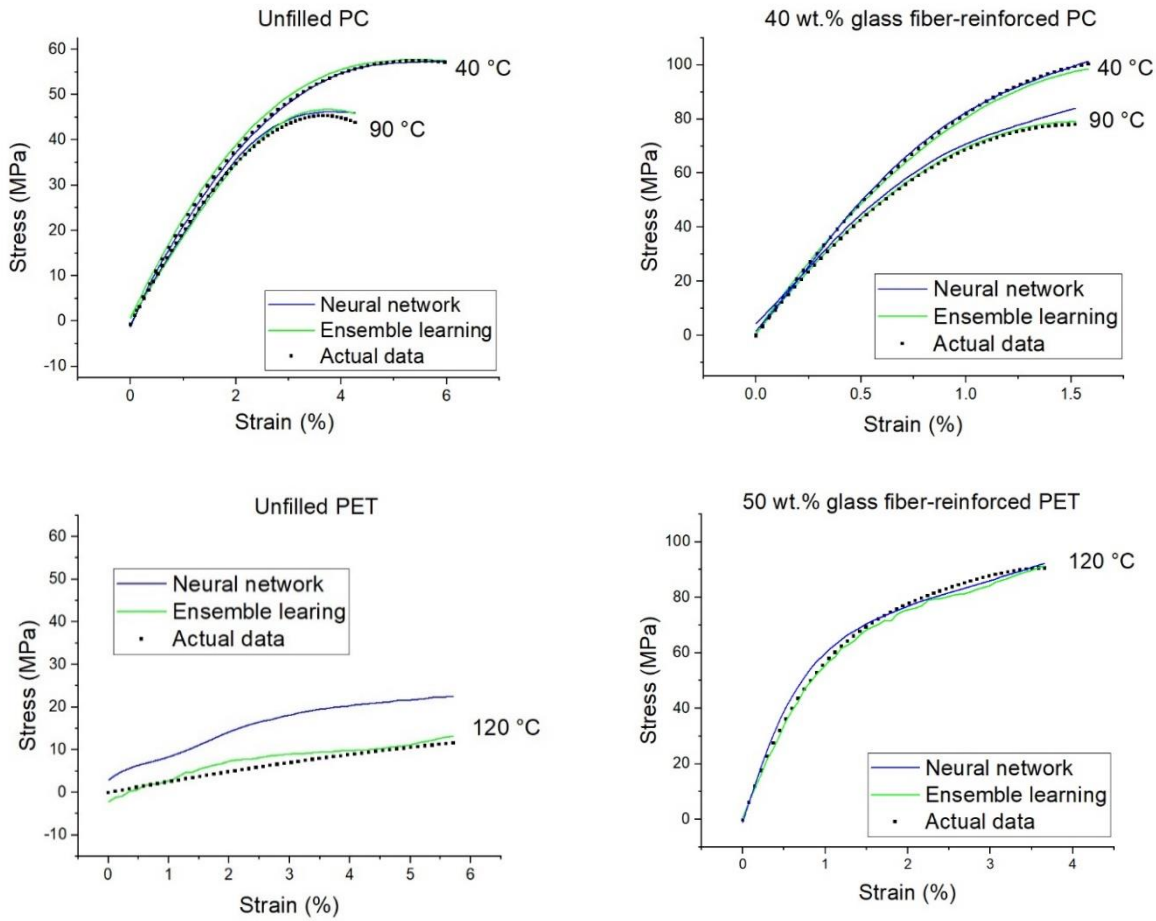

Figure 43: Predicted stress-strain curves for two selected compositions of polycarbonate (PC) and polyethylene terephthalate (PET) matrix composites based on neural networks and ensemble learning methods

Ongoing research aims to characterize fatigue and creep properties of thermoplastic composites based on data-driven approaches. The outcomes of this study will pave the way for automated design and characterization of composites, which in turn reduce the number of experiments and promote sustainability in the design and testing life cycle of a product.

7.2.1 REFERENCES

[23] Absolute Reports Pvt. Ltd. (2023). 2023-2028 Global Thermoplastic Composites Market Growth Report, MarketWatch Press Release, https://www.marketwatch.com/press-release/2023-2028-global-thermoplastic-composites-market-growth-report-2023-03-27.

[24] Rutuja, D, Eswara, P. (2021). Thermoplastic Composites Market. Applied Market Research. https://www.alliedmarketresearch.com/thermoplastic-composites-market-A11057.

[25] Red, C. (2014). Thermoplastics in Aerospace Composites Outlook, 2014-2023. Composites World. https://www.compositesworld.com/articles/the-outlook-for-thermoplastics-in-aerospace-composites-2014-2023.

7.3 A Comparative Study of Composite Delamination Modelling Under Quasi-Static Loading Conditions Using VCCT, CZM, XFEM, and the Explicit FE Scheme

G. Qi, H. Liu, NRC Aerospace; I. Y. Kim, Queen's University

It is well-known that delamination is one of the dominant failure modes in fibre-reinforced composites as it can substantially decrease the stiffness and strength of composites, leading to catastrophic structural failures. As such, accurate predictive modelling and simulation approaches are essential for understanding the delamination failure mechanism. Furthermore, a reliable modelling strategy of delamination is required to develop a holistic composite progressive failure model under general mixed-mode loading conditions, where both composite interlaminar and intralaminar failure modes are present and interact with each other. As the partial research outcome of a project in the Aerospace Future Initiative (AFI) program at the National Research Council of Canada (NRC), a comparative study is conducted to examine the effectiveness and efficiency of several commonly used interlaminar fracture modelling techniques with the finite element (FE) method. This effort aims to substantiate and consolidate the modelling methodologies and put forward recommendations for a more rational composite damage modelling practice.

Among the three fracture modes that cause delamination in a composite laminate, Mode I (opening), Mode II (in-plane shear), and a combination of both modes (mixed-mode I&II) are often found to be the dominant modes. Therefore, the widely used double cantilever beam (DCB) test, the end notched flexure (ENF) test, and the mixed-mode bending (MMB) test are carried out on unidirectional composite laminates made of carbon-fibre-reinforced epoxy prepregs (G40-800/5276-1). Besides characterizing the laminate delamination behavior under Mode I, Mode II, and mixed-mode (I & II) static fracture loading conditions, the tests obtain the corresponding fracture toughness respectively. Subsequently, the virtual crack closure technique (VCCT), the cohesive zone modelling (CZM), and the extended finite element method (XFEM) are utilized to

build 2-D FE models of the DCB, ENF, and MMB tests. An explicit FE procedure has certain advantages for solving highly nonlinear "non-smooth" quasi-static problems that are involved in complex contact interactions, large deformations, and damage due to material stiffness degradation. Accordingly, both implicit and explicit FE schemes are also examined in this study for all three tests. Based on an empirical study, the 4-node plane strain element with reduced integration scheme (CPE4R) is selected for all the 2-D FE models. For the CZM models, the 4-node 2-D cohesive element (COH2D4) is used. Displacement boundary conditions are applied to effectively mimic the test fixture, and displacement control is employed with a linear loading approach. When conducting explicit procedures, a proper loading rate and mass scaling factor are studied carefully to avoid excessive running time while keeping the kinetic energy of the mode lower than 2% of the internal energy throughout the simulations.

The mechanical response (load-displacement curves) and the progressive delamination processes in the DCB, ENF, and MMB specimens, obtained from the FE models are compared with the coupon experimental results. In general, a good agreement is exhibited between the numerical and experimental results (shown in the Figure below), which validate the modelling strategies used in this study. Meanwhile, the advantages and drawbacks of each technique are studied from the aspects of modelling difficulty, mesh dependency, required parameters and related sensitivity, rate of convergence, solution accuracy, computational cost, as well as, their application limitations. After the evaluation, useful guidance and recommendations are provided for each composite delamination modelling technique.

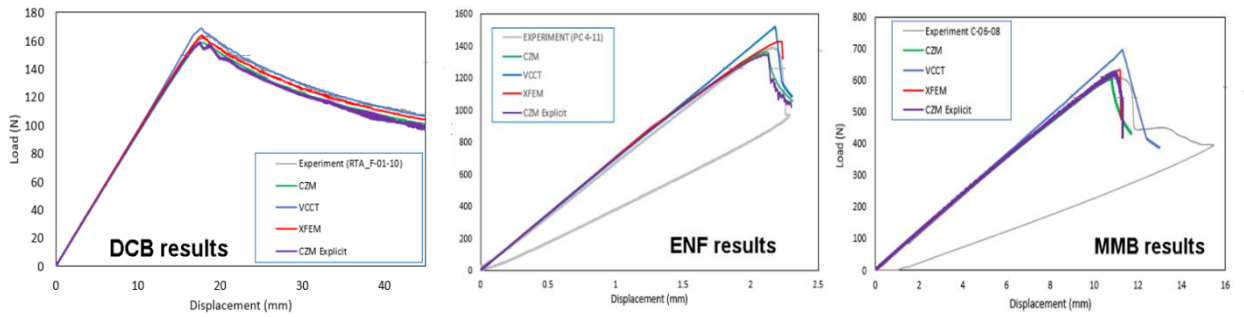

Figure 44: Comparison of load-displacement curves of DCB, ENF, MMB tests

7.3.1 REFERENCES

[26] H. Liu, G. Qi, and I. Y. Kim, "A Comparative Study of Different Damage Modelling Techniques for Composite Laminate Interlaminar Failures - A Case Study Approach", The NAFEMS World Congress 2023, Tampa, Florida, U.S., May 15-18, 2023.

[27] H. Liu, G. Qi, G. Renaud, and C. Li, "Application of the effective crack length method to model delamination

of unidirectional composite laminates under mode II shear loadings", The 25th International Conference on Composite Structures (ICCS 2022), Porto, Portugal, July 19-22, 2022.

[28] P. Shabani, C. Li, J. Laliberte, and G. Qi, "A benchmarking evaluation of finite element modelling strategies for adhesively-bonded composites using the cohesive zone modelling and virtual crack closure technique", The 8th International Conference on the Fatigue of Composites (ICFC 2021), Online Conference, June 23-25, 2021.

7.4 Analysis of Quasi-Static Mode I Delamination Growth of Double Cantilever Beam (DCB)

Gang Li, Guillaume Renaud, Lucy Li, NRC Aerospace

A study of quasi-static mode I delamination in a laminated composite double cantilever beam (DCB) configuration was conducted experimentally, analytically, and numerically [29] [30]. Using the experimentally-measured DCB compliance, the initial crack or delamination length and its propagation profile can be determined using analytical solution developed at the National Research Council of Canada (NRC). Also, a finite element (FE) correction method that consists of a series of analyses of the DCB compliances at different delamination lengths was conducted to establish an analytical correlation between the two parameters. The analytical correlation was then used to determine an effective delamination length from the experimentally measured compliance. Close agreement in the delamination lengths was obtained between the analytical solution and the FE correction method. Consequently, problematic delamination lengths received from in-situ optical measurement were corrected effectively using the two analysis procedures. Good agreement in the load-displacement variation was then obtained between the DCB FE modelling results using cohesive elements and the experimental results. The developed analytical solution is applicable without carrying out tedious numerical analyses required by the FE correction method, which should improve validation of the modelling with the testing. The DCB mode I loading, delamination length variation, FE model using cohesive elements, and comparison of the load-displacement curves obtained from tests and numerical analyses are shown in Figure 45.

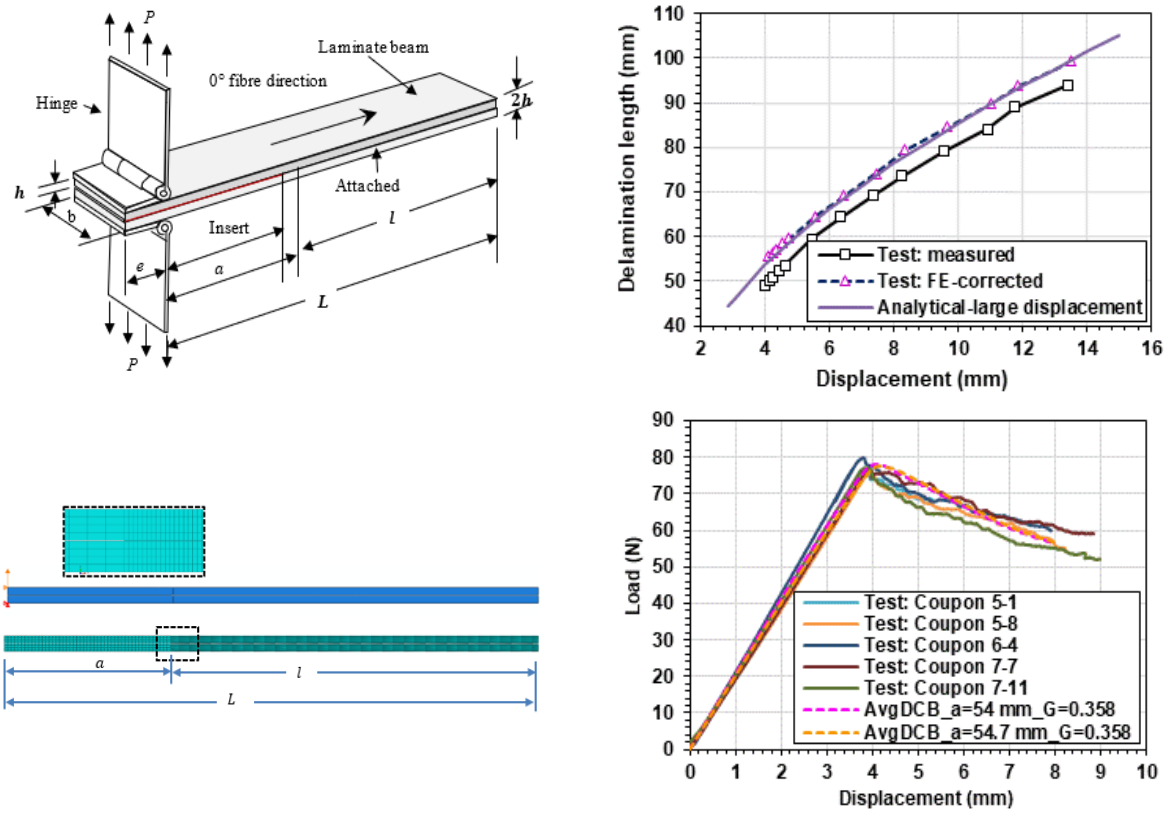

Figure 45: Schematic diagrams. Top, left and right: Laminated DCB in mode I loading and delamination-DCB opening displacement variations; Bottom, left and right: a 2D finite element model using cohesive elements and comparison of the load-displacement curves obtained from tests and numerical analyses

7.4.1 REFERENCES

[29] G. Li, G. Renaud, and C. Li (2021), "Analytical and Numerical Analyses of Mode I Double Cantilever Beam (DCB) Static Failure", NRC Technical Report, LTR-SMM-2021-0151.

[30] G. Li, and G., Renaud (2022), "Evaluation of Composite DCB Delamination Growth by Combining Experimental Data and Numerical Analysis (Paper 6), in the proceedings of 2022 American Society for Composites conference, Tucson, Arizona, Sept. 19-21, 2022.

7.5 Fatigue Simulation of Mode I Debonding in a Bonded Composite DCB Structure

Gang Li, Guillaume Renaud, NRC Aerospace

An analysis procedure was developed to evaluate and validate fatigue modelling of mode I bonded composite double-cantilever beam (DCB) coupons [31]. This work was carried out in conjunction

with theoretical analysis and experimental testing. First, an analytical solution was developed for determining the theoretical debond length based on the tested compliance of the bonded DCB opening. This analytical solution was used to evaluate and effectively correct in-situ visually measured debond lengths, which reduced the experimental scatter and improved the test results for validating finite element (FE) modelling. Three fatigue modelling approaches, two from Abaqus integrated with the virtual crack closure technique (VCCT) and one from AFGROW, were then evaluated and validated for the two available extreme test conditions, with applied displacement ratios of $R = 0.1$ and 0.7. To apply the AFGROW approach, an analytical curve for characterizing the cyclic debond growth behaviour was developed. Results also showed that the Abaqus "fatigue" modelling analysis approach generated more accurate fatigue results than the "direct cyclic" modelling approach. Very close agreement in the fatigue debond growth profiles were obtained between the test and the Abaqus "fatigue" and the AFGROW modelling approaches. Comparisons of the DCB fatigue debonding versus the number of cycles, $a - N$, curves obtained experimentally and numerically in two loading ratios are shown in Figure 46.

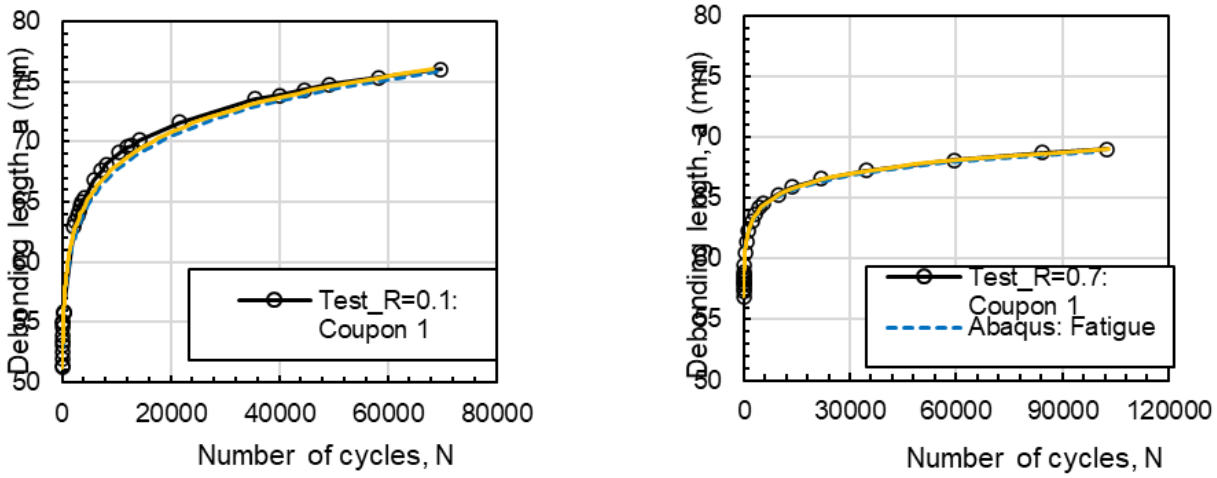

Figure 46: Comparison of fatigue $a - N$ curves obtained from tests and numerical analyses for the applied displacement ratio is: (a) $R = 0.1$ and (b) $R = 0.7$

7.5.1 REFERENCES

[31] G. Li, G. Renaud, (2022), "Modelling Fatigue Debonding in a Bonded Composite DCB Structure", NRC Technical Report, LTR-SMM-2022-0045.

7.6 High-Cycle Fatigue Modelling using Cohesive Zone Model for a Bonded Composite DCB Configuration

Gang Li, NRC Aerospace

A high-cycle fatigue modelling strategy was presented for bonded composite double-cantilever beam (DCB) specimen configuration in mode I loading [32]. This work was carried out using two-dimensional (2D) finite element (FE) modelling analysis in conjunction with cohesive zone model, damage mechanics, fracture mechanics, fatigue behaviour, user subroutine, and debond length analysis. The DCB adhesive layer was replaced by the same sized cohesive zone meshed using elements. An analysis of accumulative local fatigue damage within the cohesive elements was conducted via a correlation with global crack growth rate characterized by the Paris law. A total damage variable that consists of static and fatigue damage parameters was characterized, which was used to be a field variable in the user written subroutine for controlling degradation and failure behaviour in cohesive elements through fatigue cycles. To improve numerical analysis efficiency, an analytical method was also developed for determining debond length through fatigue cycles. Experimental validation was carried out for the two available extreme test conditions, loading ratio R = 0.1 and 0.7. Also, a numerical evaluation was conducted using an available Abaqus fatigue approach integrated with virtual crack closure technique (VCCT). Good agreement was obtained between the experimental and current numerical analyses results. Comparison of the fatigue debond propagation versus the number of fatigue cycles curves obtained from tests, current high-cycle fatigue modelling, and the available Abaqus fatigue approach are shown in Figure 47.

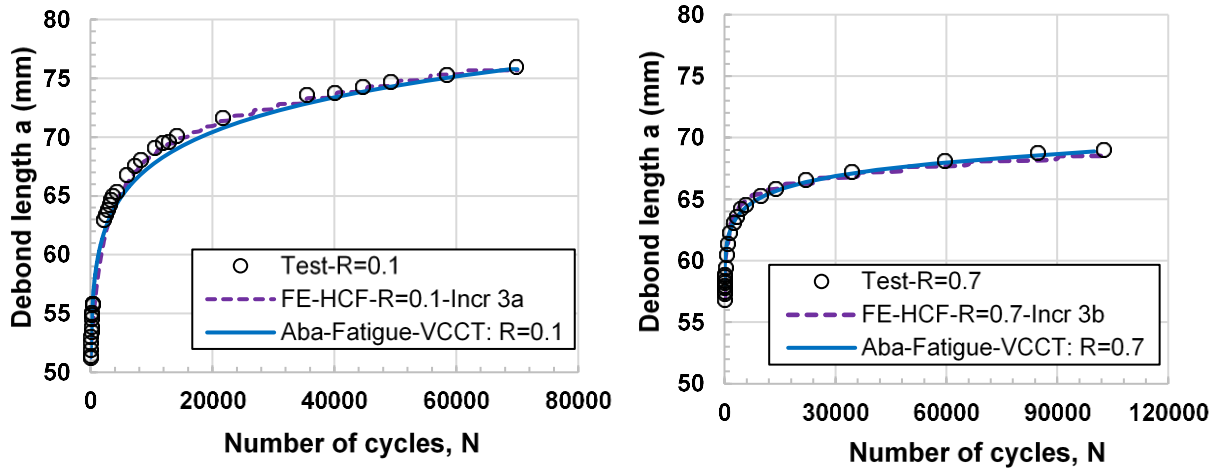

Figure 47: Comparison of fatigue $a - N$ curves obtained from tests, current high-cycle modelling approach using cohesive elements, and the available Abaqus fatigue approach integrated with VCCT for the applied displacement ratio at (a) $R = 0.1$ and (b) $R = 0.7$

7.6.1 REFERENCES

[32] G. Li (2022), "Simulation of high-cycle fatigue using cohesive zone model for a bonded composite DCB configuration", NRC Technical Report, LTR-SMM-2022-0014.

7.7 Simulation of Debond in Mixed-Mode Bending (MMB) Test Using VCCT and Cohesive Elements

Gang Li, Guillaume Renaud, NRC Aerospace

A finite element (FE) modelling strategy and a simulation performance assessment for bonded composite specimens in mixed-mode I/II loading condition was performed [33]. The quasi-static failure behaviour of the mixed-mode bending (MMB) specimen was modelled using either the virtual crack closure technique (VCCT) or cohesive zone elements. Previous NRC test data were re-examined for FE modelling validation, the measured initial debond lengths were evaluated and updated based on correlations between the initial stiffness and the debond length in the associated mode mixities. With the resulting "effective" initial debond lengths and proper mixed-mode analysis setups, the FE models generated predictions that were validated using test results. The performance of VCCT and cohesive elements was assessed over a wide range of mode mixities (0.2, 0.4, 0.6, and 0.8). Good predictions were generated using VCCT through all the assessed mode mixities, which could not be obtained from the models using cohesive zone elements. The test setup of the bonded MMB specimen and comparisons of the load-displacement curves obtained experimentally and numerically in two mixity loadings are shown in Figure 48.

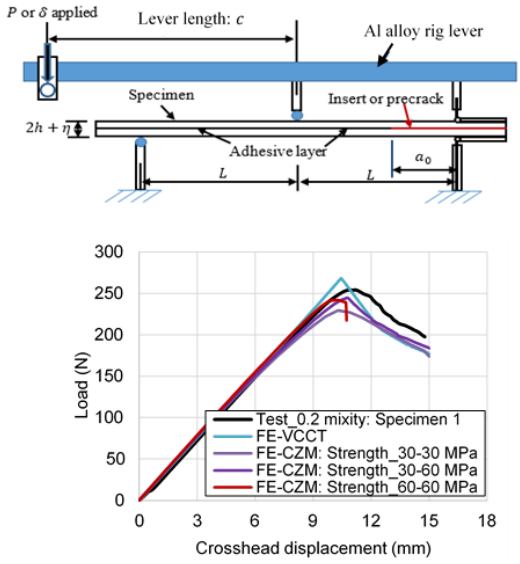

Figure 48: Top: MMB specimen test setup; Bottom: comparison of P-δ curves obtained from test and numerical analyses for the 0.2 mode mixity condition

7.7.1 REFERENCES

[33] G. Li, G. Renaud (2023), "Simulation of Mixed-Mode I/II Debond Using VCCT and Cohesive Elements", Paper 004451 submitted to 2023 American Society for Composites Conference, September 17-20, 2023 in Greater Boston, Massachusetts, USA.

7.8 Fatigue Behaviour Analysis of Mode II ENF and Mixed-mode MMB Specimens

Gang Li, Guillaume Renaud, NRC Aerospace

A two-step analysis procedure was proposed to study experimental fatigue behaviors and the associated numerical modelling of bonded ASTM composite specimens under mode II and mixed-mode loadings [34][35]. In this procedure, step 1 was to characterize the fatigue debonding and the associated loading conditions through raw data analysis; variations in the applied cyclic forces and displacements were investigated over cycles. The measured debond lengths were evaluated and converted to "effective" lengths using a correlation between the debond length and the experimental compliance determined by elimination of nonlinearity effect. According to the actual loading ratio variation, proper fatigue propagation were characterized using Paris law. Also, sound test databases were generated to support numerical analyses. Step 2 was to present an applicable FE modelling and analysis methodology using virtual crack closure technique (VCCT) based on the sound test databases obtained from the step 1. Also, another modelling tool, AFGROW, was used to simulate the fatigue debond growth. Good agreement in the debond propagation versus fatigue cycles, a vs. N, variations was obtained between the test and the two numerical analyses approaches. AFGROW could well replicate the test fatigue lives. Also, good agreement in the load versus fatigue cycles, P vs. N, was obtained between the test and FE analysis. The study shows that the presented two-step analysis procedure and its associated methodologies are of practical effectiveness and versatility. Variations of actual loading ratios and fatigue debond growth rates used from a mode II ENF specimen and a MMB specimen in 0.2 mode mixity loadings are shown in Figure 49.

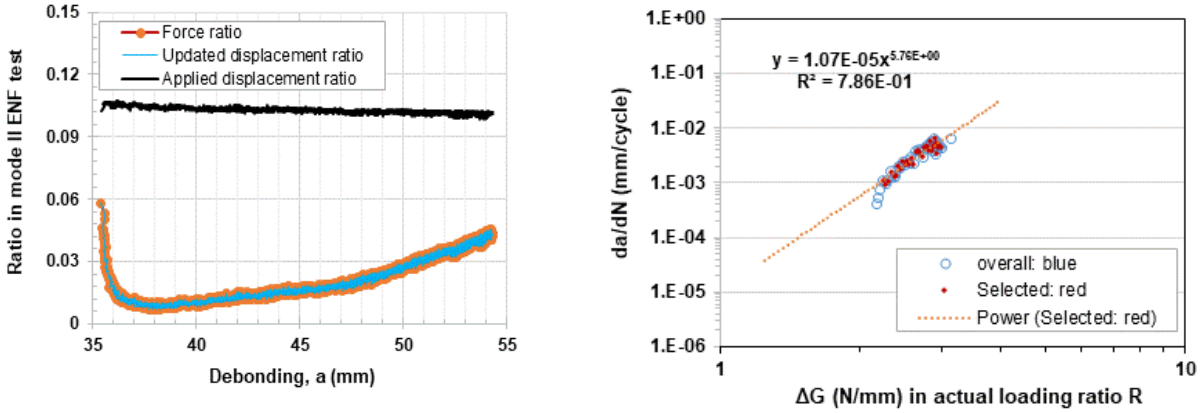

(a)

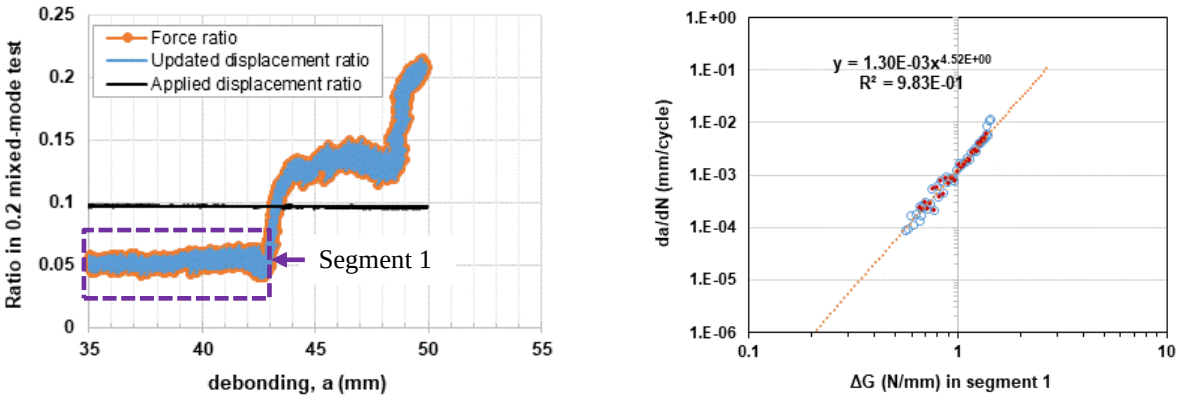

(b)

Figure 49: Variations of actual loading ratio and debond fatigue growth rate tested under (a) mode II and (b) mixed-mode I/II of 0.2 mixity conditions; where the red data dots were characterized using Paris law for the fatigue behavior assessment

7.8.1 REFERENCES

[34] G. Li, and G. Renaud (2023), "Modelling and Simulation of Fatigue Debonding in Mode II and Mixed-Mode I/II loadings", NRC Technical Report, LTR-SMM-2023-0061.

[35] G. Li, G. Renaud, C. Li, and M. Liao (2023), "Fatigue Testing and Modelling of Bonded Composite Specimens in Mode I, II, and Mixed-Mode I/II Loading", the 21st International ASTM/ESIS Symposium of Fatigue and Fracture Mechanics, Nov. 8-10, 2023, Washington, DC, USA.

8.0 FATIGUE AND STRUCTURAL INTEGRITY OF NEW MATERIALS AND MANUFACTURING

8.1 Fatigue Life Prediction of a Novel Aluminum Alloy using Intrinsic Fatigue Toughness

S.S. Dash and D.L. Chen, Department of Mechanical and Industrial Engineering, Toronto Metropolitan University, Canada.

Fatigue life assessment was performed on a newly developed vacuum-assisted high pressure die cast Al-10%Si alloy with a low Fe content [36]. This specific alloy named Silafont®-36 alloy has potential applications in the automotive and aerospace industries due to its superior combination of strength and elongation, along with good castability and treatability, etc. Although the alloy possessed good static properties, there were no earlier studies in the open literature on the dynamic fatigue behavior. Strain-controlled fatigue tests under fully-reversed cycling were performed on the cast Silafont®-36 alloy at Toronto Metropolitan University in collaboration with Shanghai Jiao Tong University [36]. The alloy consisted of a heterogenous microstructure with primary Al dendrites and fibrous Al-Si eutectic structure [37], which exhibited a good fatigue resistance. Figure 50 shows some typical low-cycle fatigue results obtained for this alloy at different total strain amplitudes.

Figure 50 (a) shows the symmetrical stress-strain hysteresis loops at mid-life depicting a near-Masing behavior of the alloy. Increase in the stress amplitude with increasing number of cycles demonstrated the cyclic hardening characteristics in this cast alloy for total strain amplitudes ≥ 0.2% (Figure 50(b)). While fatigue life of this alloy was comparable with those of several other Al-Si alloys at lower strain amplitudes (Figure 50(c)), it had a superior fatigue life at higher strain amplitudes. The fatigue life increased upon decreasing the applied total strain amplitudes. A new method for determining the intrinsic fatigue toughness (W_o) was proposed on the basis of the strain-energy density (i.e., the area under the stress-strain hysteresis loops) until failure, which accounted for the cyclic damage in the material. The fatigue life was then predicted nicely via the strain-energy density based model involving the W_o, the mid-life strain-energy density (W_m), and other parameters from the well-known Coffin-Manson-Basquin model like the cyclic strain hardening exponent (n') and fatigue ductility coefficient (c). The fatigue life predicted in this way was in

good agreement with the experimental life and lay in-between the results obtained via other methods as shown in Figure 50(d).

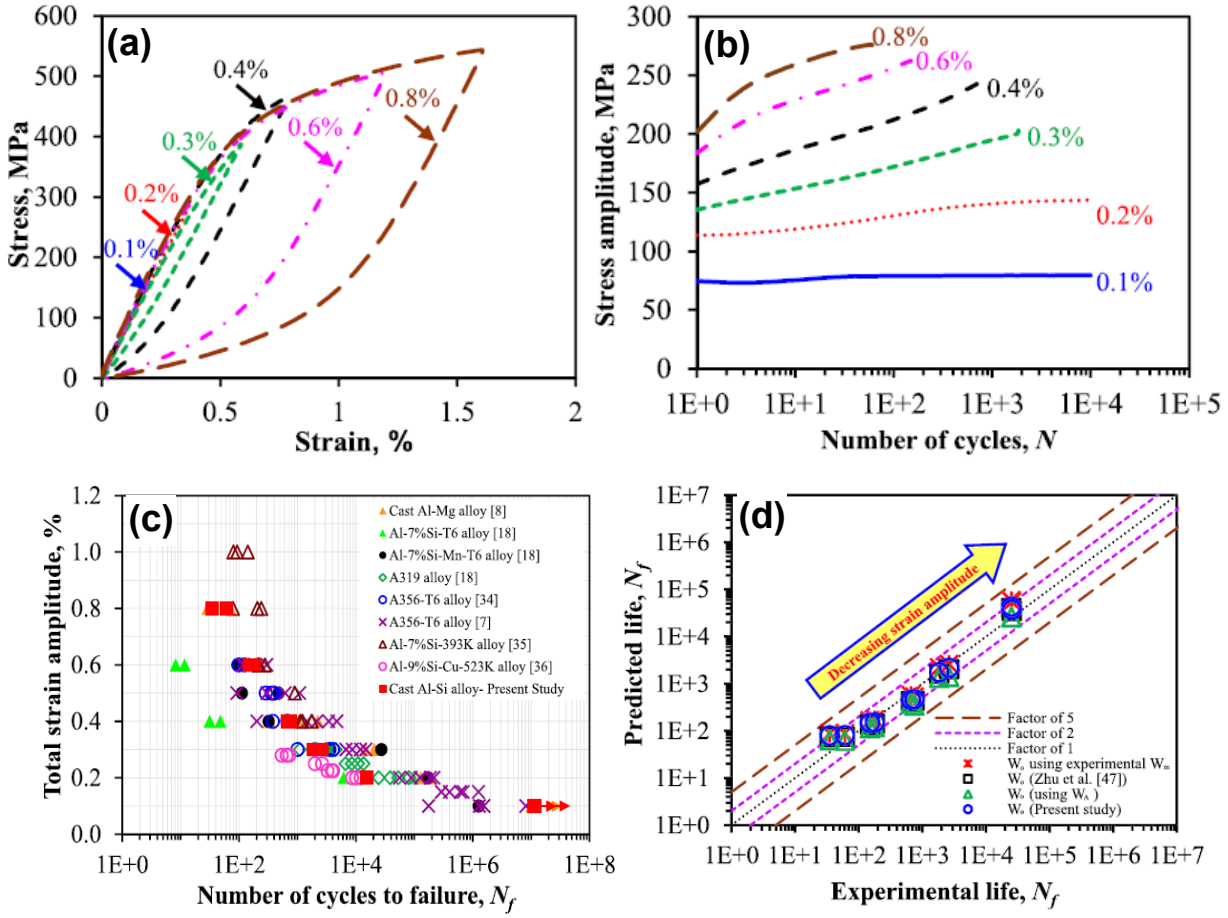

Figure 50: (a) Typical hysteresis loops at various total strain amplitudes of cast Silafont®-36 alloy; (b) evolution of the stress amplitude with the number of cycles (*N*) at various total strain amplitudes; (c) fatigue life of cast Silafont®-36 alloy in comparison with those reported in the literature; (d) predicted vs. experimental fatigue life of the alloy using a new model presented in [36]

8.1.1 REFERENCES

[36] S.S. Dash, D.J. Li, X.Q. Zeng, D.Y. Li, D.L. Chen, Cyclic deformation behavior and fatigue life prediction of an automotive cast aluminum alloy: A new method of determining intrinsic fatigue toughness, Fatigue Fract. Eng. Mater. Struct. 45 (2022) 725–738. https://doi.org/10.1111/ffe.13629.

[37] S.S. Dash, D.J. Li, X.Q. Zeng, D.L. Chen, Heterogeneous microstructure and deformation behavior of an automotive grade aluminum alloy, J. Alloys Compd. 870 (2021) 159413. https://doi.org/10.1016/j.jallcom.2021.159413.

8.2 Effect of Mean Strain on Low-Cycle Fatigue Behavior of an Aluminum-Silicon Alloy

S.S. Dash and D.L. Chen
Department of Mechanical and Industrial Engineering, Toronto Metropolitan University, Canada

Cyclic deformation behavior of a newly-developed cast Al-Si alloy was investigated under symmetric and asymmetric loading conditions [38]. The cast Silafont®-36 alloy showed superior fatigue behavior under fully-reversed, i.e., strain ratio, $R_\varepsilon = -1$, compared to some other commercially used Al-Si alloys [39]. The objective of this study was to understand the fatigue deformation mechanisms under a wide range of mean strains and especially under negative strain ratios, ranging from minus infinity ($-\infty$) to +0.5. Fatigue life of structural alloys has been estimated using various damage and energy-accumulation based or empirical equation (Basquin and Coffin-Manson relations) based approaches. However, these models do not account for the asymmetrical loading conditions which are common in any real-life situations. Analyzing the mean stress relaxation involved in strain-controlled low-cycle fatigue loading with different R_ε values is important to better understand the fatigue deformation mechanisms of alloys.

Figure 51 (a) shows the stress-strain hysteresis loops at different strain ratios and a fixed total strain amplitude of 0.4%, which became increasingly more asymmetric when the strain ratio was deviated more from $R_\varepsilon = -1$. A newly-proposed slope method was used to calculate the degree of cyclic hardening (D_{ch}^*) for the alloy under different strain ratios as shown in Figure 51 (b). While cyclic hardening occurred evidently throughout the entire cyclic deformation process at all the strain ratios for this alloy, the degree of cyclic hardening increased with decreasing strain ratio. The fatigue life of the alloy was slightly lower at positive strain ratios, with its maximum value obtained at zero mean strain (or $R_\varepsilon = -1$). In the negative range of strain ratios ($R_\varepsilon < -1$), the fatigue life increased slightly with increasing strain ratio. Mean stress relaxation was observed for all the strain ratios except $R_\varepsilon = -1$, as shown in Figure 51 (c). A new power-law based empirical equation was proposed to describe the concave nature of mean stress relaxation at negative strain ratios below −1, while a polynomial function to the power of two was used to express the trajectory of mean stress relaxation with a convex shape at zero and positive strain ratios (Figure 51 (d)). Both equations were observed to fit the experimental data nicely, with a coefficient of determination being close to 1 in all cases. The study also demonstrated that the intrinsic fatigue toughness was a material constant, which was not affected by the strain ratio under the strain-controlled low-cycle fatigue condition.

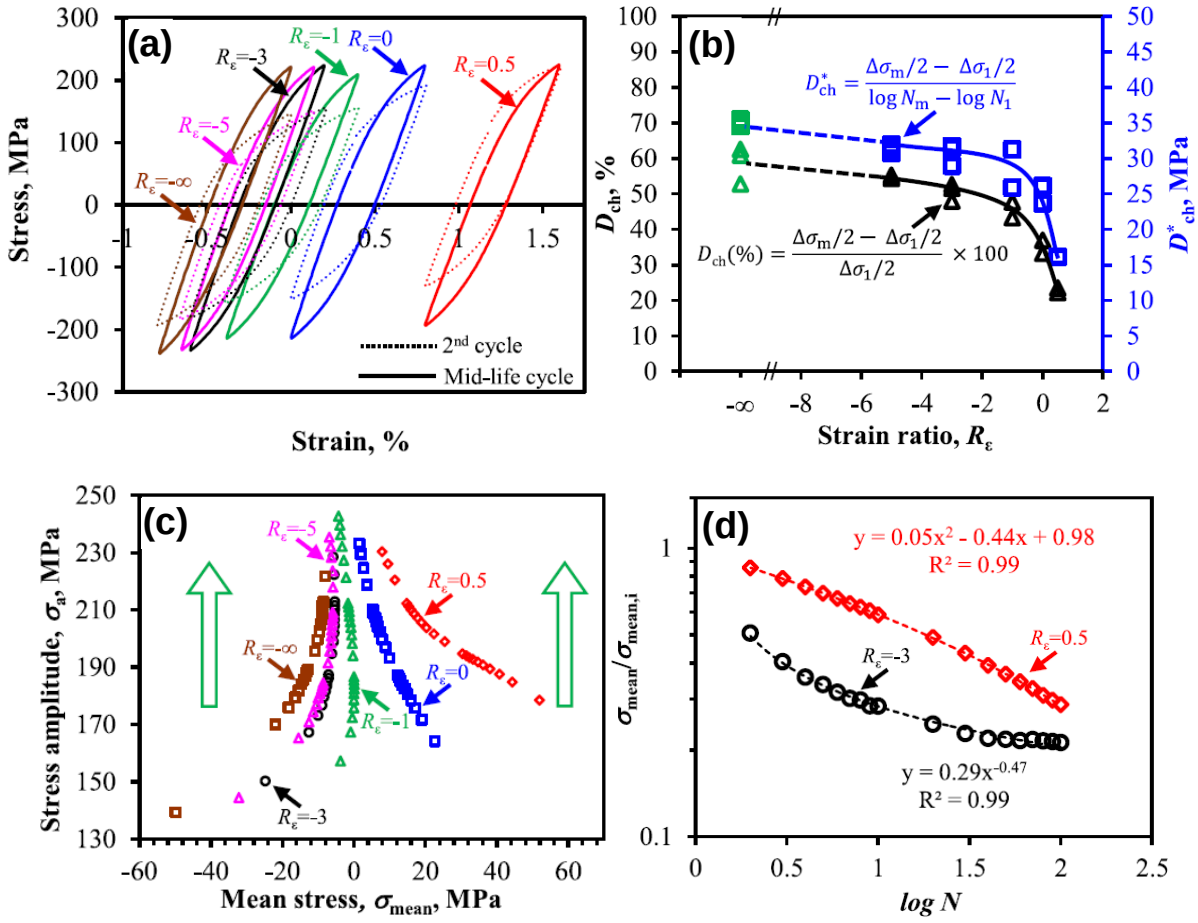

Figure 51: (a) Stress-strain hysteresis loops at different strain ratios and a fixed total strain amplitude of 0.4% for the second and mid-life cycles in the cast Silafont®-36 alloy; (b) degree of cyclic hardening based on two definitions vs. strain ratio for cast Silafont®-36 alloy; (c) evolution of the stress amplitude vs. mean stress for all recorded cycles; (d) normalized mean stress vs. logarithm of number of cycles (*N*) to establish empirical relationships for the mean stress relaxation phenomenon

8.2.1 REFERENCES

[38] S. S. Dash, D. J. Li, X. Q. Zeng, D. Y. Li, and D. L. Chen, "Low-cycle fatigue behavior of Silafont®-36 automotive aluminum alloy: Effect of negative strain ratio," Mater. Sci. Eng. A, vol. 852, p. 143701, Aug. 2022, doi: 10.1016/j.msea.2022.143701.

[39] S. S. Dash, D. J. Li, X. Q. Zeng, D. Y. Li, and D. L. Chen, "Cyclic deformation behavior and fatigue life prediction of an automotive cast aluminum alloy: A new method of determining intrinsic fatigue toughness," Fatigue Fract. Eng. Mater. Struct., vol. 45, no. 3, pp. 725–738, Mar. 2022, doi: 10.1111/ffe.13629.

8.3 Breaking Through the Limits of Ceramics with Biomimicry

H. Yazdani Sarvestani, Backman, D., Genest, M., Gholipour, J., Wanjara, P., Patnaik, P., Ashrafi, B., NRC Aerospace

Combining strength, toughness, impact resistance, and high temperature resistance in ceramics is a major engineering challenge with important applications in defense, transportation, aerospace, robotics, and energy. Architectured materials and interfaces offer promising design strategies to enhance the strength and toughness of brittle ceramics, enabling impact-resistant structures with tunable properties [40]. Humans have used the concept of architectured materials with weak interfaces since ancient times, particularly in stone walls, arches, domes, and lamellar armors. Recent developments in bio-inspired architectured materials have led to the creation of architectured ceramics, in which the building blocks are individual layers of material bonded by weaker interfaces. Several studies at the National Research Council Canada have showed that bioinspired architectured ceramics outperform plain ceramics in quasi-static and impact conditions [40]-[45].

Based on a study undertaken on beetles, we have developed helicoidal ceramics, and proved their superior biomechanical functionalities by demonstrating the role of helicoidal architectures in providing enhanced stress redistribution and energy absorption over a conventional design when subjected to compressive loading. Also, we have drawn inspiration from natural materials, such as nacre and conch shell, as well as, the American white pelican feather and dragonfly wing to architect ceramic systems with stochastic designs. These ceramics were manufactured by stacking laser-engraved/cut architectured ceramic tiles and commercially-available monomer Surlyn (see Figure 52). The mechanics of these multilayered architectured ceramics was investigated both numerically and experimentally by subjecting them to out-of-plane quasi-static and impact loads. Digital image correlation, computed radiography technique, micro-CT scanning and 3D laser scanning microscopy were used for multiscale damage assessment during and after loading [3-4]. However, when using biomimetic designs as prototypes for optimization, the design space is too large for efficient exploration via an empirical approach; thus, we propose a new approach to architecting these materials using machine learning, trained with a database of hundreds of validated structures derived from finite element analysis.

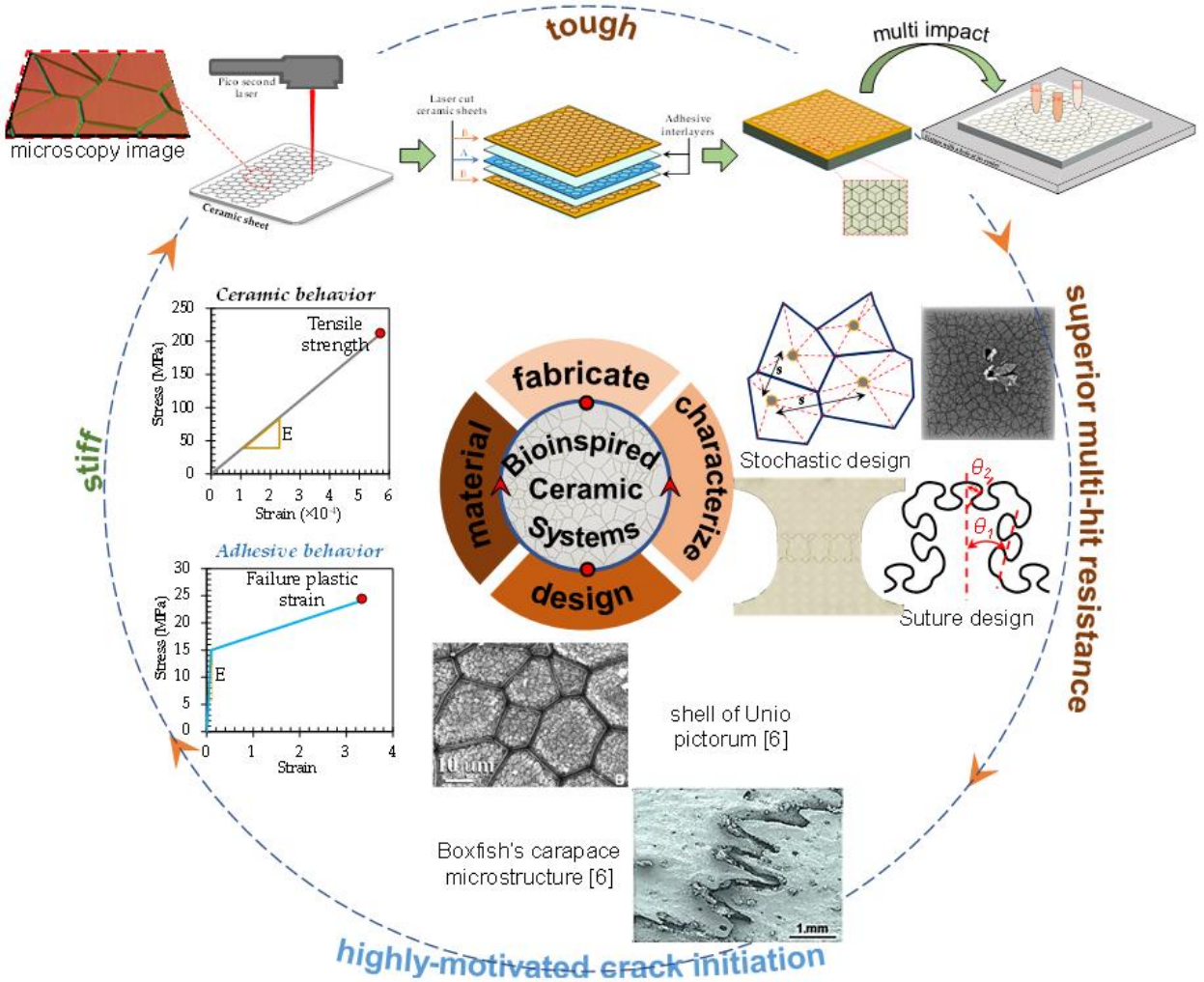

Figure 52: Manufacturing steps of the multilayered bioinspired ceramics: laser machining ceramic tiles and simplified lamination, design and arrangement of material architectures

8.3.1 REFERENCES

[40] Sarvestani, H.Y., Beausoleil, C., Genest, M. and Ashrafi, B., 2020. Architectured ceramics with tunable toughness and stiffness. Extreme Mechanics Letters, 39, p.100844.

[41] Yazdani Sarvestani, H., Aranguren van Egmond, D., Esmail, I., Genest, M., Paquet, C. and Ashrafi, B., 2022. Bioinspired stochastic design: tough and stiff ceramic systems. Advanced Functional Materials, 32(6), p.2108492.

[42] Rahimizadeh, A., Sarvestani, H.Y., Li, L., Robles, J.B., Backman, D., Lessard, L. and Ashrafi, B., 2021. Engineering toughening mechanisms in architectured ceramic-based bioinspired materials. Materials & Design, 198, p.109375.

[43] Katz, Z., Yazdani Sarvestani, H., Baradari, J.G. and Ashrafi, B., 2023. Bioinspired Hierarchical Ceramic Sutures for Multi-Modal Performance. Advanced Materials Interfaces.

[44] Sarvestani, H.Y., Mirkhalaf, M., Akbarzadeh, A.H., Backman, D., Genest, M. and Ashrafi, B., 2019. Multilayered architectured ceramic panels with weak interfaces: Energy absorption and multi-hit capabilities. Materials & Design, 167, p.107627.

[45] Rajabi, H., Ghoroubi, N., Malaki, M., Darvizeh, A. and Gorb, S.N., 2016. Basal complex and basal venation of Odonata wings: structural diversity and potential role in the wing deformation. PLoS One, 11(8), p.e0160610.

8.4 A Model for Predicting the Fatigue Life of Functionally Graded Additively Manufactured Metal Components

Captain Francis Pantuso, CD, MEng, rmc, Royal Canadian Air Force, Royal Military College of Canada (RMC)

The localized control of material properties within a complex geometry through additive manufacturing is an opportunity for improving the performance of metal aerospace components. The practical significance of this capability is that conventional components may be replaced with functionally graded components, achieving greater fatigue life than the original, while maintaining the same form and function. Similarly, new components could be designed that outperform ungraded components. In both cases the maintenance burdens; e.g., time between replacement and inspection requirements, are reduced resulting in a cost savings and an increase in operational availability of aerospace systems. A notched specimen representative of a common feature of aerospace components was selected and is shown in Figure 53. Two example cases were analyzed: functionally graded microstructure using electron beam powder bed fusion (E-PBF) and Ti-6Al-4V material feedstock, and functionally graded material composition using directed energy deposition (DED) grading from Ti-6Al-4V to 7075-T6. The grading was defined mathematically using a potential function that relates the desired functional grading to the normalized length in the direction of crack growth L. All examples assumed constant amplitude loading with a stress ratio of R = 0.1.

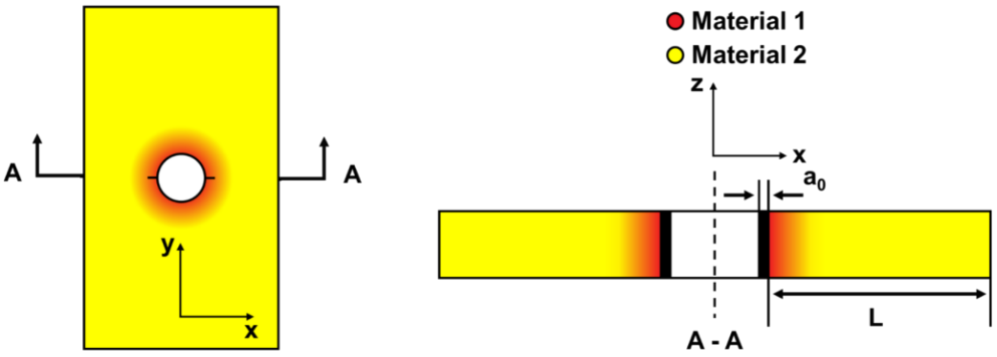

Figure 53: Custom graded specimen with potential function

Using conventional fatigue life analysis, a model was developed to estimate the crack initiation and crack growth of the example cases. Crack initiation was modelled by assigning experimentally determined material parameters for additive manufactured materials available in the literature and by applying a mean-stress corrected strain-life equation. Crack growth was modelled by adjusting the material crack growth rate between the two materials being graded according to the value of the potential function. Results comparing the crack growth life of an ungraded specimen and a specimen of graded Ti-6Al-4V laths is shown in Figure 54a. Results comparing the total fatigue life (crack initiation and crack growth) of an ungraded 7075-T6 specimen and a specimen graded with Ti-6Al-4V strengthening the notch and then transitioning to 7075-T6 is shown in Figure 54b. All results are theoretical estimates of fatigue life. Testing of E-PBF Ti-6Al-4V specimens manufactured with different process parameters is currently ongoing. Strain-life data for E-PBF Ti-6Al-4V were taken from Radlof et al. [46] and Zhang et al. [47]. Crack growth rate data for E-PBF Ti-6Al-4V were taken from Seifi et al [48] and Galarraga et al. [49].

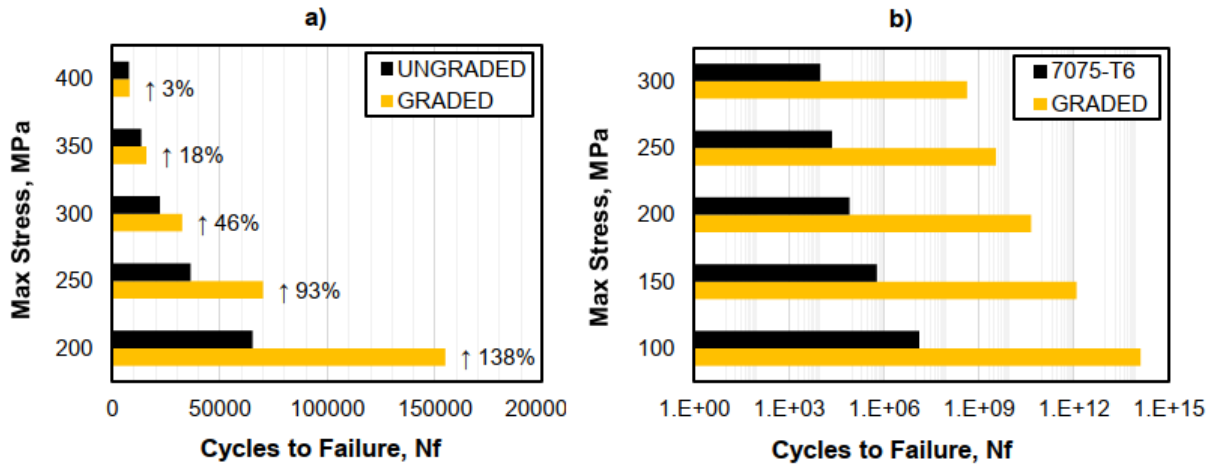

Figure 54: Crack growth life comparison where a) compares an ungraded E-PBF Ti-6Al-4V to a specimen of graded E-PBF Ti-6Al-4V alpha laths, and b) compares total crack life between an ungraded 7075-T6 specimen and a graded specimen with Ti-6Al-4V strengthening near the notch graded to 7075-T6 using DED

8.4.1 REFERENCES

[46] Radlof, W., Benz, C., Heyer, H., and Sander, M. "Monotonic and Fatigue Behavior of EBM Manufactured Ti-6Al-4V Solid Samples: Experimental, Analytical and Numerical Investigations." Materials 2020, Vol. 13, Page 4642, Vol. 13, No. 20, 2020, p. 4642. https://doi.org/10.3390/MA13204642.

[47] Zhang, Y., Chen, Z., Qu, S., Feng, A., Mi, G., Shen, J., Huang, X., and Chen, D. "Multiple Sub-Variants and Anisotropic Mechanical Properties of an Additively-Manufactured Ti-6Al-4V Alloy." Journal of Materials Science & Technology, Vol. 70, 2021, pp. 113–124. https://doi.org/10.1016/j.jmst.2020.06.039.

[48] Seifi, M., Salem, A., Satko, D., Shaffer, J., and Lewandowski, J. J. "Defect Distribution and Microstructure Heterogeneity Effects on Fracture Resistance and Fatigue Behavior of EBM Ti–6Al–4V." International

Journal of Fatigue, Vol. 94, 2017, pp. 263–287. https://doi.org/10.1016/J.IJFATIGUE.2016.06.001.

[49] Galarraga, H., Warren, R. J., Lados, D. A., Dehoff, R. R., and Kirka, M. M. "Fatigue Crack Growth Mechanisms at the Microstructure Scale in As-Fabricated and Heat Treated Ti-6Al-4V ELI Manufactured by Electron Beam Melting (EBM)." 2017. https://doi.org/10.1016/j.engfracmech.2017.03.024.

8.5 Progress Towards the Certification of Additively Manufactured Primary Structural Components for Aerospace Applications

David Backman, Priti Wanjara, Sheida Sarafan, Javad Gholipour and Sila Atabay, NRC Aerospace

One of the key aspects to bring additively manufactured structural parts into mainstream aviation use is the ability to certify these parts as airworthy. This project update details the results of a certification like test approach taken for additively manufactured, Ti-6Al-4V corner fittings (brackets) – produced using electron beam melting (Arcam Q20 plus technology) – for the CP-140 Aurora aircraft.

During the reporting period, a methodology was developed for evaluating the location dependence of the tensile mechanical properties of the corner fitting part by extracting sub-sample coupons from the as-built and hot isostatically pressed (HIP'd) brackets for metallographic examination, hardness mapping, tensile testing and fractography. The sub-sample coupon hardness results showed variability in the different regions of the as-built CP-140 bracket with the right and left wall [see Figure 55] of the bracket base showing larger variations in hardness. Sub-sample hardness testing of a Hot Isotatically Pressed [HIP] bracket showed less variability in hardness. Follow up tensile testing of unHIP'd (i.e. as-built) sub-sample specimens showed an average elastic modulus of 121 GPa with an average elongation at failure of 2.0%. The HIP'd sub-sample coupons showed a similar elastic modulus with a substantially improved average elongation at failure of 15.3%. From fractographic examination, HIP'ing of the bracket was seen as an effective method to heal the lack of fusion defects present in the as-built bracket and thereby significantly improve the elongation.

For component-level testing of the additively manufactured corner fittings, the first bracket (B1) was as-machined and subjected to a static overload; the second (B2) and third (B3) brackets were as-machined and subjected to only standard static loading; and the fourth bracket (B4) was HIP'd and also subjected to only standard static loading. In all cases, the brackets were considered to have passed "certification" with the first three brackets (B1, B2, B3) lasting over four (4) lifetimes of fatigue loading. The fourth bracket (B4) subjected to the HIP process lasted almost 10 lifetimes of fatigue loading. Table 2 provides summary results of the overall bracket testing. Fractographic results showed a similar fatigue failure location for brackets B2 to B4, with crack nucleation occurring in the rear of the bracket [see Figure 56]. The first bracket (B1) subjected to overload,

did not suffer a fatigue failure, with the test stopping due to a failure in the fastener securing the bracket to the test fixture. A deeper analysis of the test results, suggested that the overload condition oversized the fastener holes on the bracket and changed the loading distribution, resulting in the failure of the fastener.

Overall, the test results showed that the electron beam melting process was able to produce high quality, certifiable parts in both the as-machined and HIP'd conditions.

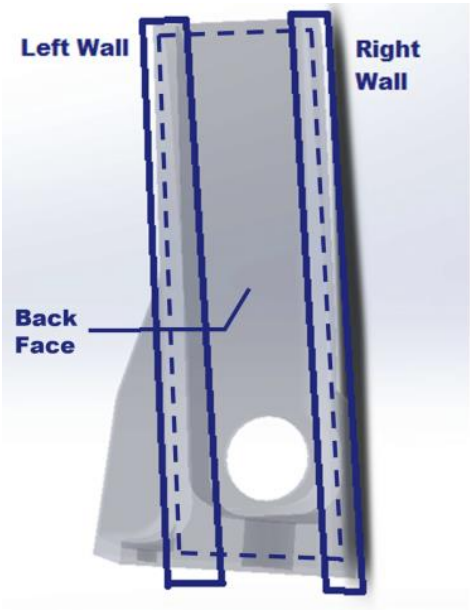

Figure 55: Diagram indicating how each bracket was cut into the three main samples that were examined

Table 2: Summary of bracket certification like testing

	Bracket 1 (unHIP'd)	Bracket 2 (unHIP'd)	Bracket 3 (unHIP'd)	Bracket 4 (HIP'd)
Static Overload	Passed	N/A	N/A	N/A
Static Load	Passed	Passed	Passed	Passed
Fatigue Spectrum (2 Full Lifecycles)	Passed	Passed	Passed	Passed
Final Failure	LC5 BL1	LC4 BL7	LC4 BL4	LC10 BL8
Failure Mode	Bolt	Bracket	Bracket	Bracket

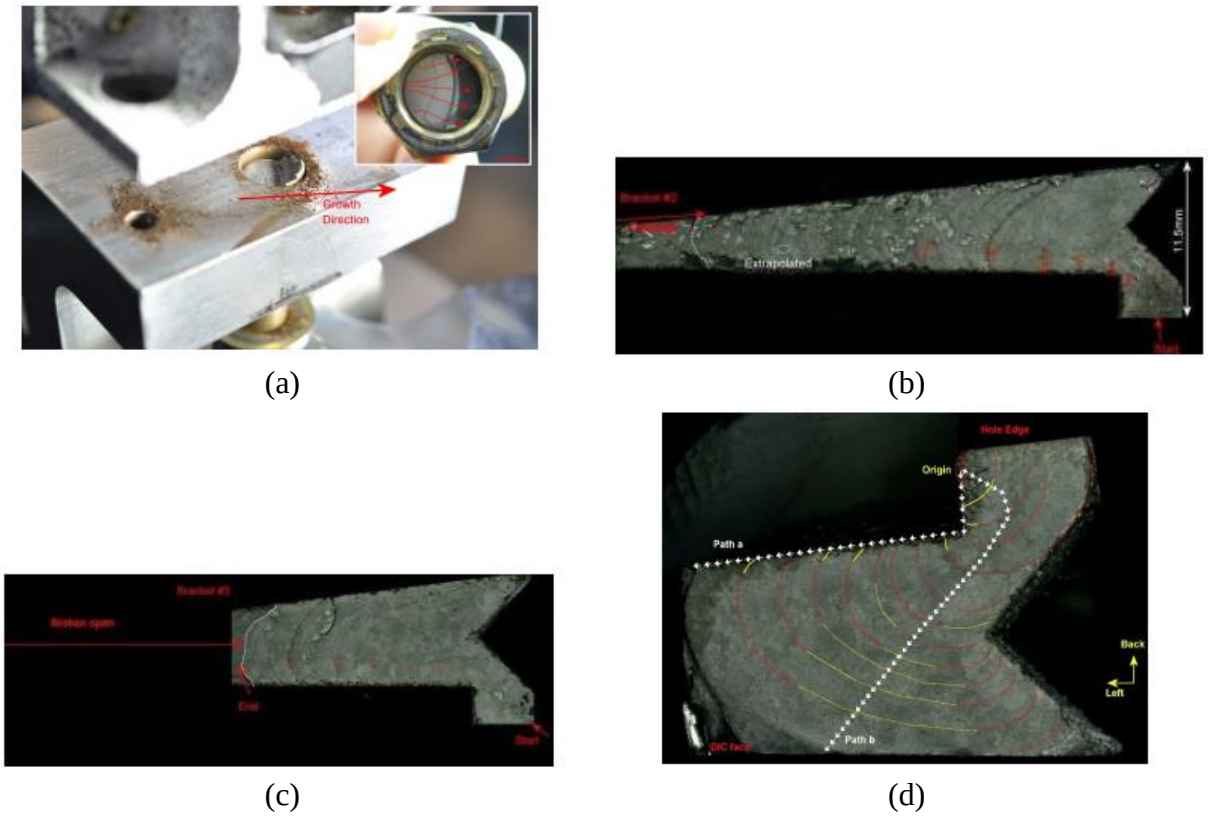

(a) (b)

(c) (d)

Figure 56: (a) Bracket 1 fracture surface (large bolt) and direction of crack propagation (b) Bracket 2 fracture surface (right wall) and direction of crack propagation (c) Bracket 3 fracture surface (right wall) and direction of crack propagation (d) Bracket 4 fracture surface (right wall) and direction of crack propagation

8.5.1 REFERENCE

[50] D. Backman, J.H. Sa, S. Jain, P. Wanjara, S. Sarafan, J. Gholipour, S. Atabay, and R. Desnoyers, Certification Testing of Additively Manufactured CP-140 Corner Fittings, LTR-SMM-2022-0122, August 2022.

9.0 ACKNOWLEDGEMENTS

The NRC Aerospace Strategic Client Service Program "*Defence Technologies and Sustainment (DTS)*" provided support for the NRC's effort to prepare for this ICAF National Review.

Special thanks to all the organizations and authors who have contributed various inputs to the Canadian National Review for ICAF2023.

Special thanks to Dr. Shashank Pants and Dr. Guillaume Renaud for reviewing/commenting on this report.